binding properties of NFATc2 and NFATc1 to the IL-2 and TNF-α promoters by using a ChIP assay. As shown in Fig. 6, almost the same amounts of the IL-2 and TNF-α promoter regions were coprecipitated with ectopically expressed NFATc2 as well as NFATc1 in Jurkat Tag cells upon stimulation. These results suggest that the selective defect of NFATc1 in up-regulation of TNF-α was not because of lack of binding activity for the TNF-α promoter/enhancer region.

Discussion

The differential contribution of NFATc2 and NFATc1 to TNF-α gene transcription has been suggested by a reporter assay and an in vitro DNA binding assay (15, 18, 19). This study revealed that NFATc2, but not NFATc1, promoted TNF-α synthesis in human peripheral $CD4^+$ T cells. This is generally consistent with previous reports that TNF-α synthesis by lymphocytes and/or T cells was impaired in NFATc2$^{-/-}$ mice (9) but not in NFATc1$^{-/-}$ mice (8). Furthermore, our present results demonstrating that the enhancement of TNF-α expression by NFAT was lost by the truncation of TAD2 and that NFATc2-TAD2 specifically suppressed NFAT-TNF-α activity clearly suggest that TAD2 is required for NFAT-mediated transactivation of the TNF-α gene but not the IL-2 gene.

It has been demonstrated that the full response at many NFAT sites requires concomitant activation of the AP-1 transcription factor family (1, 33). There is a discernible AP-1 site immediately downstream of the NFAT sites in the promoter region of IL-2 and other cytokine genes. Furthermore, the three-dimensional structures of NFATc2-DBD, AP-1 heterodimer (Jun/Fos), and the distal Ag-receptor response element in the IL-2 gene promoter, which we used as NFAT-IL-2 in this study, have been analyzed in detail (34). The importance of NFAT/AP-1 cooperativity in gene regulation was revealed by studies demonstrating that mutations of the AP-1-interacting domain of NFATc2 led to loss of transactivation of many cytokine genes, including IL-2 (35). Deletion of either the NFAT site or the AP-1 site is sufficient to destroy IL-2 promoter activity (36).

In contrast, the association of NFAT with the consensus sequence for a NFκB-binding site spanning −106 to −87 in the TNF-α gene promoter (κ3 site, which we used as NFAT-TNF-α in this study) is essential for TNF-α expression in T cells (37–39). Unlike the case of IL-2, Macian et al. (35) demonstrated that cooperation with AP-1 is not crucial for NFAT-dependent transactivation of the TNF-α gene. Cooperation with the Jun/ATF2 heterodimer, but not with AP-1 (Jun/Fos), is required for full induction of TNF-α expression by NFAT (30–32), although the Jun/ATF2-interacting region in NFAT has not been identified. In contrast to NFAT-IL-2 on which NFAT contacts AP-1 via its DBD, the following evidence suggests the possibility that NFAT interacts with Jun/ATF2 or other undefined coactivators on NFAT-TNF-α through TAD2. First, TAD2 was crucial for NFAT-dependent transactivation of the TNF-α gene (Fig. 3). Second, TAD2 behaved as a dominant negative against the transcriptional activity of NFAT-TNF-α, but not against that of NFAT-IL-2 (Fig. 5*B*). In addition, NFATc2 and NFATc1 equivalently associated with NFAT-TNF-α in vivo (Fig. 6). Nevertheless, Jun/ATF2-dependent transcriptional activity was not affected by NFATc2-TAD2 (Fig. 5*B*). Therefore, NFAT may cooperate with other factors than Jun/ATF2 in activating NFAT-TNF-α; otherwise, similar to the case of NFAT/AP-1 complex (34), strong interaction between NFAT and Jun/ATF2 may require their target DNA sequences. To elucidate additional details of the contribution of TAD2 to NFAT-TNF-α activation, analysis of the cocrystallized structure of the complex of transcription factors, including NFAT, on NFAT-TNF-α may be required as performed for the NFAT/AP-1/NFAT-IL-2 complex (34).

However, in disagreement with our present findings (Fig. 6), it has been reported that binding activity for NFAT-TNF-α was detectable in nuclear extracts of NFATc2- but not NFATc1- or NFATc3-transfected COS cells (18). In addition, Oum et al. (19), using in vitro DNA-protein binding assay and a reporter assay with HeLa cells, demonstrated that the functional disparity between NFATc2 and NFATc1 in the activation of TNF-α was due to the different binding specificity of NFATc2 and NFATc1 to NFAT-TNF-α. The reason for the discrepancy is unclear; our present data using NFATc2/NFATc1 chimeric molecules (Fig. 3) further support the notion that TAD2 rather than DBD predominantly contributes to the difference in TNF-α transactivation activity between NFATc2 and NFATc1. The condition in which the transcription complex was formed in vivo might not have been completely reproducible in the in vitro binding assay. Furthermore, interaction of transcription factors with their corresponding sequences may have differed among the cell types used. In fact, Monticelli et al. (40) reported that the association of NFATc1 with the murine IL-13 promoter was different between Th2 cells and mast cells. Therefore, our results showing that NFATc2 and NFATc1 equivalently associated with NFAT-TNF-α, demonstrated in T cells by ChIP assay, seem to be relatively reliable even though the physiological association between endogenous NFAT and the TNF-α promoter was too weak to further confirm this in our experimental conditions (data not shown).

In agreement with the notion that TAD2 is required for NFAT-TNF-α activation, positive participation of longer forms of NFATc1, which have TAD2, in TNF-α expression was suggested by the fact that reductions of all three NFATc1 isoforms by RNAi resulted in slight suppression of TNF-α, whereas the introduction of Stealth RNAi oligo, which down-regulated the shortest form of NFATc1 alone, failed to do so (Fig. 4). We also observed that TNF-α expression was enhanced by the longest NFATc1 isoform, although its potency was relatively weaker than that of NFATc2 (Fig. 3). These findings are partly consistent with a previous report demonstrating that the potency of NFATc.β, which has medium-length TAD2, to enhance NFAT-TNF-α activity was very low (15) and suggesting that the contribution of TAD2 derived from NFATc1 to TNF-α expression is smaller than that of NFATc2-TAD2. The essential domain in NFAT-TAD2 for its transactivation activity has not been fully elucidated. Imamura et al. (29) demonstrated that 15 amino acids, DITLDDVNEIIGRDM, in the C-terminal end of NFATx1 are required for its maximum transactivation activity in Jurkat T cells. In that region, the first 12 amino acids, DITLDDVNEIIG, are conserved in NFATc2$_{904-915}$ as well as NFAT1c/C$_{909-920}$. Exchange of the remaining three amino acids in NFATc2 (KEF) and NFATc1-c1-c1/C (NDL) little suppressed and enhanced, respectively, their transactivation activity, suggesting that the corresponding region is responsible for the differential participation of the TAD2 of NFATc2 and NFATc1/C origins. Because the effects of exchange were weak, the existence of another unknown region in TAD2 contributing to the transactivation activity is also suggested. Further examination will be required to elucidate the differential roles of TAD2 derived from NFATc2 and NFATc1/C in detail. Above all, NFATc1, especially its major and inducible shorter form, potentially contributes to the clonal expansion of activated T cells through IL-2 synthesis, but not to TNF-α-mediated exacerbation of inflammation.

Differential effects of NFATc2 and NFATc1 on the expression of IL-13 were also observed, although GM-CSF expression was enhanced by both NFATs (Fig. 2). These findings are consistent with previous reports demonstrating that the effect of NFATc1 on IL-13 gene transcription was weaker than that of NFATc2, even though this was shown in mast cells rather than Jurkat cells (40). Accordingly, IL-13 expression in mast cells was unchanged in

NFATc1$^{-/-}$ mice (40). In the report of Macian et al. (35), augmentation of the promoter activity of IL-2 and GM-CSF by mutant NFATc2, which was unable to interact with AP-1, was weaker than that by wild-type NFATc2 even though the effects of both NFATc2s on TNF-α and IL-13 were equivalent. Similar to the case of IL-2, GM-CSF promoter activity was diminished by truncation of the AP-1 binding region neighboring the NFAT site (41). Taking these findings together with our present results, it is likely that NFATc1 activates GM-CSF in cooperation with AP-1, although TAD2 is required for transactivation of the IL-13 gene by NFAT through association with other cofactors. Because no sequence completely matching the NFAT-binding region in the TNF-α promoter was detectable in the 5′-flanking region of the IL-13 gene, the mechanisms by which NFATc1 fails to enhance IL-13 expression need to be further investigated.

In conclusion, TAD2 is required for NFAT-mediated transactivation of the TNF-α gene in T cells. NFATc1, especially its shortest isoform that lacks TAD2 and is predominantly induced upon cell activation, may play characteristic roles in immune responses through its specific activation of distinct cytokines. Our present findings will be useful for developing selective TNF-α inhibitors that will be promising drugs for treating autoimmune diseases, including rheumatoid arthritis.

Acknowledgments

We thank Drs. N. Arai and K. Arai for providing human NFAT cDNAs and M. Suzuki and Y. Fujiishi for technical assistance.

Disclosures

The authors have no financial conflict of interest.

References

1. Rao, A., C. Luo, and P. G. Hogan. 1997. Transcription factors of the NFAT family: regulation and function. *Annu. Rev. Immunol.* 15: 707–747.
2. Serfling, E., F. Berberich-Siebelt, S. Chuvpilo, E. Jankevics, S. Klein-Hessling, T. Twardzik, and A. Avots. 2000. The role of NF-AT transcription factors in T cell activation and differentiation. *Biochim. Biophys. Acta* 1498: 1–18.
3. Hogan, P. G., L. Chen, J. Nardone, and A. Rao. 2003. Transcriptional regulation by calcium, calcineurin, and NFAT. *Genes Dev.* 17: 2205–2232.
4. Liu, J., J. D. Farmer, W. S. Lane, J. Friedman, I. Weissman, and S. L. Schreiber. 1991. Calcineurin is a common target of cyclophilin-cyclosporin A and FKBP-FK506 complexes. *Cell* 66: 807–815.
5. Clipstone, N. A., and G. R. Crabtree. 1992. Identification of calcineurin as a key signaling enzyme in T-lymphocyte activation. *Nature* 357: 695–697.
6. Fruman, D. A., C. B. Klee, B. E. Bierer, and S. J. Burakoff. 1992. Calcineurin phosphatase activity in T lymphocytes is inhibited by FK506 and cyclosporin A. *Proc. Natl. Acad. Sci. USA* 89: 3686–3690.
7. Ranger, A. M., M. R. Hodge, E. M. Gravallese, M. Oukka, L. Davidson, F. W. Alt, F. C. de la Brousse, T. Hoey, M. Grusby, and L. H. Glimcher. 1998. Delayed lymphoid repopulation with defects in IL-4-driven responses produced by inactivation of NF-ATc. *Immunity* 8: 125–134.
8. Yoshida, H., H. Nishina, H. Takimoto, L. E. Marengere, A. C. Wakeham, D. Bouchard, Y. Y. Kong, T. Ohteki, A. Shahinian, M. Bachmann, et al. 1998. The transcription factor NF-ATc1 regulates lymphocyte proliferation and Th2 cytokine production. *Immunity* 8: 115–124.
9. Hodge, M. R., A. M. Ranger, F. Charles de la Brousse, T. Hoey, M. J. Grusby, and L. H. Glimcher. 1996. Hyperproliferation and dysregulation of IL-4 expression in NF-ATp-deficient mice. *Immunity* 4: 397–405.
10. Kiani, A., J. P. Viola, A. H. Lichtman, and A. Rao. 1997. Down-regulation of IL-4 gene transcription and control of Th2 cell differentiation by a mechanism involving NFAT1. *Immunity* 7: 849–860.
11. Viola, J. P., A. Kiani, P. T. Bozza, and A. Rao. 1998. Regulation of allergic inflammation and eosinophil recruitment in mice lacking the transcription factor NFAT1: role of interleukin-4 (IL-4) and IL-5. *Blood* 91: 2223–2230.
12. Schuh, K., B. Kneitz, J. Heyer, F. Siebelt, C. Fischer, E. Jankevics, E. Rude, E. Schmitt, A. Schimpl, and E. Serfling. 1997. NF-ATp plays a prominent role in the transcriptional induction of Th2-type lymphokines. *Immunol. Lett.* 57: 171–175.
13. Erb, K. J., T. Twardzik, A. Palmetshofer, G. Wohlleben, U. Tatsch, and E. Serfling. 2003. Mice deficient in nuclear factor of activated T-cell transcription factor c2 mount increased Th2 responses after infection with *Nippostrongylus brasiliensis* and decreased Th1 responses after mycobacterial infection. *Infect. Immun.* 71: 6641–6647.
14. Northrop, J. P., S. N. Ho, L. Chen, D. J. Thomas, L. A. Timmerman, G. P. Nolan, A. Admon, and G. R. Crabtree. 1994. NF-AT components define a family of transcription factors targeted in T-cell activation. *Nature* 369: 497–502.
15. Park, J., A. Takeuchi, and S. Sharma. 1996. Characterization of a new isoform of the NFAT (nuclear factor of activated T cells) gene family member NFATc. *J. Biol. Chem.* 271: 20914–20921.
16. Lyakh, L., P. Ghosh, and N. R. Rice. 1997. Expression of NFAT-family proteins in normal human T cells. *Mol. Cell. Biol.* 17: 2475–2484.
17. Chuvpilo, S., M. Zimmer, A. Kerstan, J. Glockner, A. Avots, C. Escher, C. Fischer, I. Inashkina, E. Jankevics, F. Berberich-Siebelt, et al. 1999. Alternative polyadenylation events contribute to the induction of NF-ATc in effector T cells. *Immunity* 10: 261–269.
18. Ho, S. N., D. J. Thomas, L. A. Timmerman, X. Li, U. Francke, and G. R. Crabtree. 1995. NF-ATc3, a lymphoid-specific NFATc family member that is calcium-regulated and exhibits distinct DNA binding specificity. *J. Biol. Chem.* 270: 19898–19907.
19. Oum, J. H., J. Han, H. Myung, M. Hleb, S. Sharma, and J. Park. 2002. Molecular mechanism of NFAT family proteins for differential regulation of the IL-2 and TNF-α promoters. *Mol. Cells* 13: 77–84.
20. Wu, Y., M. Borde, V. Heissmeyer, M. Feuerer, A. D. Lapan, J. C. Stroud, D. L. Bates, L. Guo, A. Han, S. F. Ziegler, et al. 2006. FOXP3 controls regulatory T cell function through cooperation with NFAT. *Cell* 126: 375–387.
21. Adachi, S., Y. Amasaki, S. Miyatake, N. Arai, and M. Iwata. 2000. Successive expression and activation of NFAT family members during thymocyte differentiation. *J. Biol. Chem.* 275: 14708–14716.
22. Miyoshi, H., U. Blomer, M. Takahashi, F. H. Gage, and I. M. Verma. 1998. Development of a self-inactivating lentivirus vector. *J. Virol.* 72: 8150–8157.
23. Nagai, T., K. Ibata, E. S. Park, M. Kubota, K. Mikoshiba, and A. Miyawaki. 2002. A variant of yellow fluorescent protein with fast and efficient maturation for cell-biological applications. *Nat. Biotechnol.* 20: 87–90.
24. Karin, M., and R. I. Richards. 1982. Human metallothionein genes: primary structure of the metallothionein-II gene and a related processed gene. *Nature* 299: 797–802.
25. Kaminuma, O., M. Deckert, C. Elly, Y.-C. Liu, and A. Altman. 2001. Vav-Rac1-mediated activation of the c-Jun N-terminal kinase/c-Jun/AP-1 pathway plays a major role in stimulation of the distal NFAT site in the interleukin-2 gene promoter. *Mol. Cell. Biol.* 21: 3126–3136.
26. Van Dam, H., M. Duyndam, R. Rottier, A. Bosch, L. de Vries-Smits, P. Herrlich, A. Zantema, P. Angel, and A. J. van der Eb. 1993. Heterodimer formation of cJun and ATF-2 is responsible for induction of c-jun by the 243 amino acid adenovirus E1A protein. *EMBO J.* 12: 479–487.
27. Van Dam, H., S. Huguier, K. Kooistra, J. Baguet, E. Vial, A. J. van der Eb, P. Herrlich, P. Angel, and M. Castellazzi. 1998. Autocrine growth and anchorage independence: two complementing Jun-controlled genetic programs of cellular transformation. *Genes Dev.* 12: 1227–1239.
28. Kaminuma, O., F. Kitamura, N. Kitamura, M. Miyagishi, K. Taira, K. Yamamoto, O. Miura, and S. Miyatake. 2004. GATA-3 suppresses IFN-γ promoter activity independently of binding to *cis*-regulatory elements. *FEBS Lett.* 570: 63–68.
29. Imamura, R., E. S. Masuda, Y. Naito, S. Imai, T. Fujino, T. Takano, K. Arai, and N. Arai. 1998. Carboxyl-terminal 15-amino acid sequence of NFATx1 is possibly created by tissue-specific splicing and is essential for transactivation activity in T cells. *J. Immunol.* 161: 3455–3463.
30. Tsai, E. Y., J. Yie, D. Thanos, and A. E. Goldfeld. 1996. Cell-type-specific regulation of the human tumor necrosis factor α gene in B cells and T cells by NFATp and ATF-2/JUN. *Mol. Cell. Biol.* 16: 5232–5244.
31. Tsai, E. Y., J. Jain, P. A. Pesavento, A. Rao, and A. E. Goldfeld. 1996. Tumor necrosis factor α gene regulation in activated T cells involves ATF-2/Jun and NFATp. *Mol. Cell. Biol.* 16: 459–467.
32. Falvo, J. V., A. M. Uglialoro, B. M. Brinkman, M. Merika, B. S. Parekh, E. Y. Tsai, H. C. King, A. D. Morielli, E. G. Peralta, T. Maniatis, et al. 2000. Stimulus-specific assembly of enhancer complexes on the tumor necrosis factor α gene promoter. *Mol. Cell. Biol.* 20: 2239–2247.
33. Jain, J., P. G. McCaffrey, V. E. Valge-Archer, and A. Rao. 1992. Nuclear factor of activated T cells contains Fos and Jun. *Nature* 356: 801–804.
34. Chen, L., J. N. Glover, P. G. Hogan, A. Rao, and S. C. Harrison. 1998. Structure of the DNA-binding domains from NFAT, Fos and Jun bound specifically to DNA. *Nature* 392: 42–48.
35. Macian, F., C. Garcia-Rodriguez, and A. Rao. 2000. Gene expression elicited by NFAT in the presence or absence of cooperative recruitment of Fos and Jun. *EMBO J.* 19: 4783–4795.
36. Boise, L. H., B. Petryniak, X. Mao, C. H. June, C.-Y. Wang, T. Lindsten, R. Bravo, K. Kovary, J. M. Leiden, and C. B. Thompson. 1993. The NFAT-1 DNA binding complex in activated T cells contains Fra-1 and JunB. *Mol. Cell. Biol.* 13: 1911–1919.
37. Goldfeld, A. E., P. G. McCaffrey, J. L. Strominger, and A. Rao. 1993. Identification of a novel cyclosporin-sensitive element in the human tumor necrosis factor α gene promoter. *J. Exp. Med.* 178: 1365–1379.
38. Goldfeld, A. E., E. Tsai, R. Kincaid, P. J. Belshaw, S. L. Schrieber, J. L. Strominger, and A. Rao. 1994. Calcineurin mediates human tumor necrosis factor α gene induction in stimulated T and B cells. *J. Exp. Med.* 180: 763–768.
39. McCaffrey, P. G., A. E. Goldfeld, and A. Rao. 1994. The role of NFATp in cyclosporin A-sensitive tumor necrosis factor-α gene transcription. *J. Biol. Chem.* 48: 30445–30450.
40. Monticelli, S., D. C. Solymar, and A. Rao. 2004. Role of NFAT proteins in IL13 gene transcription in mast cells. *J. Biol. Chem.* 279: 36210–36218.
41. Johnson, B. V., A. G. Bert, G. R. Ryan, A. Condina, and P. N. Cockerill. 2004. Granulocyte-macrophage colony-stimulating factor enhancer activation requires cooperation between NFAT and AP-1 elements and is associated with extensive nucleosome reorganization. *Mol. Cell. Biol.* 24: 7914–7930.

Rice-based mucosal vaccine as a global strategy for cold-chain- and needle-free vaccination

Tomonori Nochi*†, Hidenori Takagi‡, Yoshikazu Yuki*†, Lijun Yang‡, Takehiro Masumura§¶, Mio Mejima*†, Ushio Nakanishi*, Akiko Matsumura*†, Akihiro Uozumi*, Takachika Hiroi||, Shigeto Morita§¶, Kunisuke Tanaka§¶, Fumio Takaiwa‡, and Hiroshi Kiyono*†**

*Division of Mucosal Immunology, Department of Microbiology and Immunology, The Institute of Medical Science, University of Tokyo, Tokyo 108-8639, Japan; †Core Research for Evolutional Science and Technology, Japan Science and Technology Corporation, Saitama 332-0012, Japan; ‡Transgenic Crop Research and Development Center, National Institute of Agrobiological Sciences, Ibaraki 305-8602, Japan; §Laboratory of Genetic Engineering, Graduate School of Agriculture, Kyoto Prefectural University, Shimogamo, Kyoto 606-8522, Japan; ¶Kyoto Prefectural Institute of Agricultural Biotechnology, Seika-cho, Kyoto 619-0244, Japan; and ||Department of Allergy and Immunology, Tokyo Metropolitan Institute of Medical Science, Tokyo 113-8613, Japan

Communicated by Roy Curtiss, Arizona State University, Tempe, AZ, April 26, 2007 (received for review February 6, 2007)

Capable of inducing antigen-specific immune responses in both systemic and mucosal compartments without the use of syringe and needle, mucosal vaccination is considered ideal for the global control of infectious diseases. In this study, we developed a rice-based oral vaccine expressing cholera toxin B subunit (CTB) under the control of the endosperm-specific expression promoter 2.3-kb glutelin *GluB-1* with codon usage optimization for expression in rice seed. An average of 30 μg of CTB per seed was stored in the protein bodies, which are storage organelles in rice. When mucosally fed, rice seeds expressing CTB were taken up by the M cells covering the Peyer's patches and induced CTB-specific serum IgG and mucosal IgA antibodies with neutralizing activity. When expressed in rice, CTB was protected from pepsin digestion *in vitro*. Rice-expressed CTB also remained stable and thus maintained immunogenicity at room temperature for >1.5 years, meaning that antigen-specific mucosal immune responses were induced at much lower doses than were necessary with purified recombinant CTB. Because they require neither refrigeration (cold-chain management) nor a needle, these rice-based mucosal vaccines offer a highly practical and cost-effective strategy for orally vaccinating large populations against mucosal infections, including those that may result from an act of bioterrorism.

mucosal immunity | protein body | oral vaccine | IgA | cholera toxin B subunit

The majority of emerging and reemerging infectious pathogens, including *Vibrio cholerae*, *Escherichia coli*, HIV, influenza virus, or coronavirus causing severe acute respiratory syndrome, invade and infect the host via the mucosal surfaces of the gastrointestinal, respiratory, and/or genitourinary tracts (1–3). Mucosal immunity forms a first line of defense by means of secretory IgA and cytotoxic T cells against epithelium-transmitted pathogens, and so it would seem important to develop vaccines that induce effective immune responses at mucosal barriers. Most current vaccines are administered by needle and syringe, generating effective antibody and cell-mediated responses in the systemic compartment, but not in mucosal sites (4). In contrast, mucosal vaccines administered either orally or nasally have been shown to be effective in inducing antigen-specific immune responses in both systemic and mucosal compartments (5–8). Because it elicits this two-layered protective immunity, mucosal vaccination is thought to be an ideal strategy for combating both emerging and reemerging infectious diseases (5–8). In fact, the Bill and Melinda Gates Foundation and the National Institutes of Health have proposed that mucosal vaccines be a focus of future vaccine development (9), a vision underlying the foundation of the Gates' research initiative, "Grand Challenges in Global Health" (9). Most traditional vaccines are not cost-effective because they cannot be stored at room temperature (RT), instead requiring that the "cold chain" be preserved en route from vaccine manufacturer to the field of vaccination (i.e., that no gap be allowed in the refrigeration) (10). The cost of preserving that cold chain for currently used vaccines is estimated at between $200 and $300 million a year (10). Further, if inappropriately processed or disposed of, the needles and syringes used for the vaccination can pose the threats of environmental contamination and second-hand spread of infectious disease. Producing vaccine antigens in plants would offer many practical advantages (11, 12). First, it would be less expensive to produce vaccine antigens in plants than via industrial fermentation. Second, there is no need to take elaborate means to purify the vaccine if it is expressed in plant tissue. Third, the plant expression system minimizes risks arising from contamination. Collectively, these advantages make a plant-based subunit vaccine not only attractive, but also practical for the propagation of mucosal vaccine on the global scale (12).

As early as 1990, Curtiss and Cardineau expressed *Streptcoccus mutans* surface protein antigen, the causative epitope for dental caries, in tobacco as a first step toward a potential plant-based mucosal vaccine (13). Since then, many vaccine antigen candidates, including bacterial diarrhea antigens, hepatitis B antigen, Norwalk virus antigen, and respiratory syncitial virus antigen, have been expressed in tobaccos or potatoes to demonstrate the feasibility of edible plant-based vaccines (14–21). However, these plant-based vaccines have remained a function of sophisticated bench-driven experiments and have not yet advanced to practical application. If such a vaccine is to be practicable for global immunization, it must be storable at RT for long periods, be protected from the harsh environment of the gastrointestinal tract, and target mucosal inductive tissues, including Peyer's patches (PPs) (8, 22).

We here introduce a rice-based oral vaccine possessing many practical advantages over most traditional or other plant-based oral vaccines. The rice-based oral vaccine is stable at RT for several years and is protected from digestive enzymes. When ingested, this vaccine induced antigen-specific antibodies with neutralizing activities. These results show that the rice-based oral vaccine offers a highly practical global strategy for cold-chain- and needle-free vaccination against infection.

Author contributions: T.N. and H.T. contributed equally to this work; T.N., Y.Y., and H.K. designed research; T.N., H.T., Y.Y., L.Y., T.M., M.M., U.N., A.M., A.U., T.H., S.M., K.T., and F.T. performed research; T.N., H.T., and Y.Y. analyzed data; and T.N., Y.Y., and H.K. wrote the paper.

The authors declare no conflict of interest.

Abbreviations: CHO, Chinese hamster ovary; CT, cholera toxin; CTB, cholera toxin B subunit; LTB, heat-labile enterotoxin B subunit; PPs, Peyer's patches; PB, protein body; RT, room temperature.

See Commentary on page 10757.

**To whom correspondence should be addressed. E-mail: kiyono@ims.u-tokyo.ac.jp.

www.pnas.org/cgi/doi/10.1073/pnas.0703766104

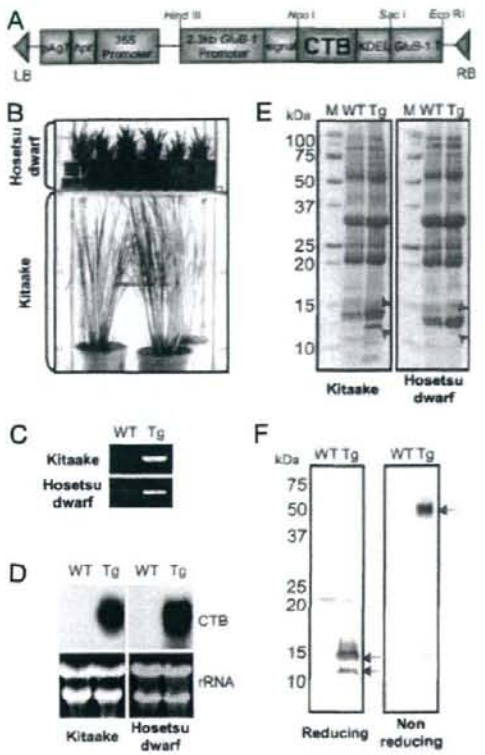

Fig. 1. Expression of CTB in transgenic rice. (*A*) T-DNA plasmid-inserted, codon-optimized CTB gene for rice seed, controlled by the rice seed storage protein glutelin 2.3-kb *GluB-1* promoter. The signal sequence of *GluB-1* and the retention signal to the endoplasmic reticulum coding KDEL are located at the N- and C-terminal regions, respectively. (*B*) The Kitaake and Hosetsu dwarf type rice strains expressed CTB in a dosed chamber. (*C*) Integration of the CTB gene into the genomic DNA was confirmed by PCR. WT, Wild-type nontransgenic rice; Tg, CTB-expressed transgenic rice. (*D*) Northern blot analysis was performed for the confirmation of CTB mRNA expression. (*E* and *F*) SDS/PAGE and Western blot analysis revealed that high levels of CTB protein were expressed in rice. Arrowheads indicate 12- and 15-kDa forms of CTB (*E*). The CTB protein, composed of two fragments, forms a 55- to 65-kDa pentamer structure under nonreducing conditions. Arrows indicate monomeric (under reducing condition) and pentamer (under nonreducing condition) forms of CTB (*F*).

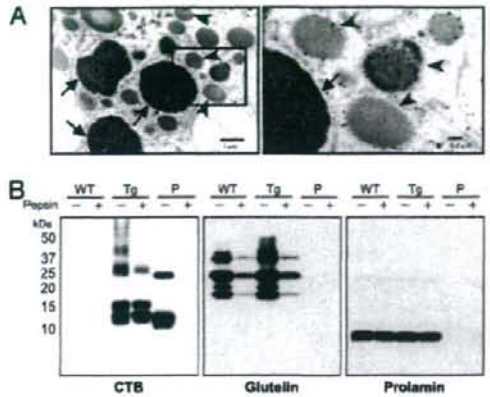

Fig. 2. Localization and digestive enzyme resistivity of rice-expressed CTB in PBs. (*A*) Data obtained through immunoelectron microscopic analysis with anti-CTB antibody. A positive signal was obtained with 20 nm of gold particles. CTB expressed in rice are stored in PB-I (arrowheads) and PB-II (arrows). (*B*) Pepsin digestion was carried out under the conditions described in *Materials and Methods*. Approximately 90% of glutelins but not 13k prolamins were digested *in vitro*, whereas ≈75% of rice-based CTB but not purified rCTB remained intact.

Results

Development of Rice-Based Mucosal Vaccine Expressing Cholera Toxin B Subunit (CTB) in Seeds. We purposely chose CTB as a prototype antigen to demonstrate both the capacity of the rice-based mucosal vaccine to induce systemic as well as mucosal immunity and to showcase the practicality of using the rice transgenic expression system. Once generated with binary vector (pGPTV-35S-HPT) (23), as described in Fig. 1*A*, codon-optimized CTB genes for rice seed were transfected into the rice plant [*Oryza sativa* L. cv Kitaake, a normal-sized rice (24); and Hosetsu, a dwarf type rice (25, 26), shown in Fig. 1*B*] by using *Agrobacterium tumefaciens*-mediated transformation (27). Hosetsu dwarf type rice, a naturally occurring gene mutant on the gibberellin biosynthesis pathway (25), is 20 cm in height and has a short life cycle (≈3 months). Genomic PCR analysis revealed that the CTB gene was integrated into the genomic DNA of both lines of rice plants (Fig. 1*C*). In addition, high levels of CTB-specific mRNA in the seeds of both lines of transgenic but not nontransgenic wild-type (WT) rice were expressed at 15 days after flowering (Fig. 1*D*). When we examined the accumulation of CTB protein in the transgenic rice seed by SDS/PAGE and Western blot analysis with anti-CTB polyclonal antibody, two bands (12 kDa and 15 kDa) were detected under denatured conditions (Fig. 1 *E* and *F*). Using densitometry analysis with rCTB as a standard, we found that expression levels of CTB reached an average of 30 μg per seed in the Kitaake strain, representing 2.1% of the total seed protein (0.15% of seed weight). The expression level of CTB in Hosetsu dwarf type rice was lower (average of 5 μg per seed) than that in Kitaake rice. Furthermore, Western blot analysis under nonreducing conditions revealed that CTB expressed in rice formed a pentamer with 55 to 65 kDa (Fig. 1*F*), indicating that most of the CTB expressed in rice seed is considered to be a functionally native form possessing the ability to bind to the GM1 ganglioside, known to be expressed at the apical surface of the intestinal epithelium and to be a receptor for CTB (28).

CTB Expressed in Protein Bodies (PBs) of Rice Seed Is Resistant to Gastrointestinal Harsh Environment. In addition to being easy to produce and administer, an effective oral vaccine would also have to have a built-in safeguard against digestion, particularly against the harsh acidic environments found in the stomach. The starchy endosperm in rice contains two types of protein storage organs, PB-I and PB-II, which are distinguished by their shape, density, and protein composition (29). The main storage proteins for PB-I are the alcohol-soluble prolamins (e.g., 13k prolamin) and the water-soluble glutelins (e.g., glutelin B1) (29, 30). Because they are water-soluble, the glutelins (PB-II) are more vulnerable to digestion in the gastrointestinal tract than are prolamins (PB-I). Immunoelectron microscopic analysis reveals that CTB is localized not only on the surface of PB-I, but also on the inside of PB-II (Fig. 2*A*). To examine the ability of the CTB accumulated in the rice PB to withstand protease digestion in the stomach, total seed proteins were subjected to pepsin treatment. Western blot analysis (Fig. 2*B*) revealed that the signal intensity of the 13k prolamin was not significantly changed by the pepsin treatment, whereas ≈90% of the glutelins were digested by pepsin under these conditions. In addition, ≈75% of the CTB accumulated in rice seed remained intact after pepsin treatment (Fig. 2*B*). These findings suggest that most

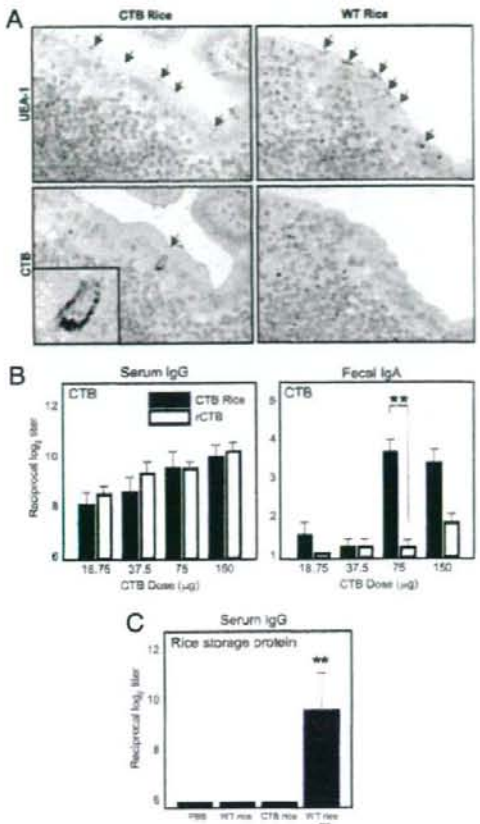

Fig. 3. Effective uptake of rice-expressed CTB by M cells for the induction of antigen-specific immune responses. (*A*) Rice-expressed CTB was administered into an intestinal loop containing PPs. Thirty minutes after the inoculation, the brisk CTBs were taken up by UEA-1-positive M cells (arrow), but not columnar epithelial cells. (*B*) When mice were orally immunized with rice-expressed CTB, purified rCTB, or nontransgenic rice dissolved in water or water alone as controls, equal levels of CTB-specific serum IgG responses were induced in mice immunized with rice-expressed CTB or purified rCTB, but not in mice receiving WT rice or water alone. In contrast, CTB-specific fecal IgA responses were also induced in mice immunized with a small amount (50 mg of seed powder containing 75 μg of CTB) of rice-expressed CTB, but not with an identical dose of purified rCTB. **, $P < 0.01$, CTB rice vs. rCTB. (*C*) Rice-expressed CTB did not induce rice storage protein-specific serum IgG responses. **, $P < 0.01$, WT rice plus CT vs. CTB rice.

of the CTB expressed in transgenic rice seed can be protected from the harsh conditions of the gastrointestinal tract. To characterize the mucosal immunogenicity of the rice-based oral vaccine in more detail, we opted to use the Kitaake CTB system for the remainder of the study.

Rice-Expressed CTB Is Effectively Taken Up by Antigen-Sampling M Cells for the Induction of Antigen-Specific Immune Responses. To confirm the M cell uptake of rice-expressed CTB, a suspension of rice-expressed CTB or nontransgenic WT rice was administered into the ligated small intestinal loops, including the PPs of naive mice. Histological analysis with *Ulex europaeus* agglutinin (UEA-1), which is a well known marker of murine M cells (31), demonstrated a strong presence of CTB antigen in UEA-1$^+$ M cells (Fig. 3*A*). We

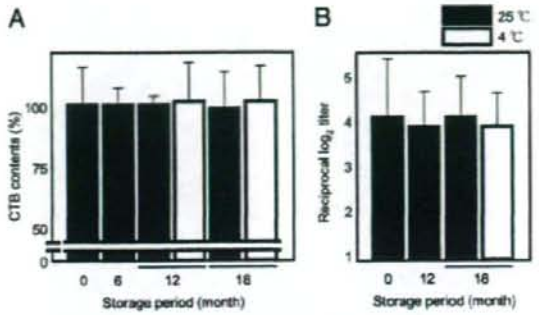

Fig. 4. Temperature stability of rice-expressed CTB. (*A*) One thousand rice seeds expressing CTB were preserved in a 500-ml sealed bottle for >1.5 years at 4°C as well as at RT (25°C). The content of CTB in preserved rice was not changed compared to that in freshly harvested rice (29 ± 4 μg per seed). (*B*) Mice were orally immunized with preserved rice-expressed CTB (50 mg of seed powder containing 75 μg of CTB) as described in Fig. 3. The preserved rice induced CTB-specific mucosal IgA responses that were comparable to those observed for freshly harvested rice.

next orally immunized mice with the seed powder of rice-expressed CTB or purified rCTB. Rice-expressed CTB induced CTB-specific serum IgG and fecal IgA antibodies (Fig. 3*B*). CTB-specific fecal IgA responses were also induced in mice immunized with a low dose of rice-expressed CTB (e.g., 50 mg of rice powder containing 75 μg CTB), whereas the same dose of purified rCTB induced no or very low levels of antigen-specific IgA responses (Fig. 3*B*). Furthermore, it should be emphasized that rice-expressed CTB induced no rice storage protein-specific immune responses (Fig. 3*C*). These findings demonstrated that the rice-based mucosal vaccine is an effective delivery vehicle for the induction of antigen-specific mucosal IgA responses.

Rice-Based Mucosal Vaccine Maintained Immunogenicity for More than 1.5 Years at RT. Inasmuch as our results provide supportive evidence for the protective advantage of rice-based mucosal vaccine, which includes stability in the harsh condition of the gastrointestinal tract (Fig. 2*B*), it was logical to examine whether the rice-based vaccine preserved at RT (25°C) for an extended period maintained its stability and mucosal immunogenicity. To this end, rice-based mucosal vaccine was preserved for 0.5, 1.0, or 1.5 years at either RT (25°C) or 4°C. Densitometry analysis revealed that the antigen in rice seed remained stable at RT for >1.5 years (Fig. 4*A*). Furthermore, the rice preserved at RT for 1.5 years induced the same level of CTB-specific fecal IgA responses as freshly harvested rice (Fig. 4*B*). These data suggest that the rice-based mucosal vaccine is more stable than the purified antigen of the subunit vaccine, as well as more effective for induction of IgA-committed mucosal immune responses.

Rice-Expressed CTB Induces Protective Immunity Against Cholera Toxin (CT). Finally, to examine the biological activities of antibodies induced by oral administration of rice-expressed CTB, CT-neutralizing activities were investigated by using a GM1-binding inhibition assay with GM1-ELISA (17) and an elongation assay with Chinese hamster ovary (CHO) cells (17, 32). When serum samples from mice orally immunized with rice-expressed CTB or WT rice were subjected to GM1-ELISA, the binding of CT to the coated GM1 ganglioside was blocked in the former but not the latter group of samples (Fig. 5*A*). The elongation assay also revealed no morphological changes in CHO cells cocultured with CT that had been pretreated with serum from mice orally vaccinated with rice-expressed CTB. In contrast, CT pretreated with

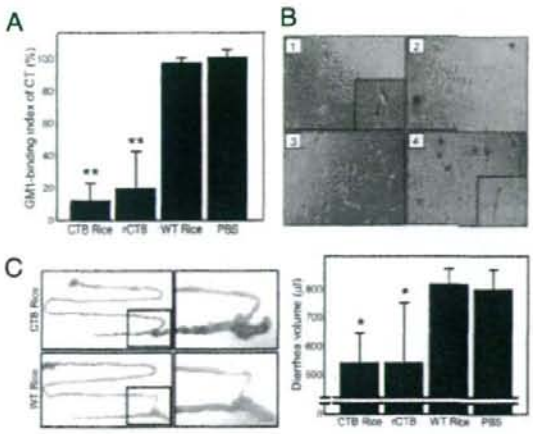

Fig. 5. Induction of protective immunity against CT by rice-expressed CTB. (*A*) The neutralizing index calculated with OD_{450} obtained by GM1-ELISA. The serum of mice immunized with rice-expressed CTB or purified rCTB, but not with nontransgenic rice or PBS, completely blocked the binding of CT to coated GM1-ganglioside. **, $P < 0.01$, CTB rice or rCTB vs. PBS. (*B*) The elongation assay with CHO cells revealed a morphology similar to normal cells (1) when the cells were stimulated with CT pretreated with serum from mice immunized with rice-expressed CTB (2) or purified rCTB (3), but a marked elongation when stimulated by CT pretreated with the serum from mice immunized with nontransgenic rice, PBS, or nontreated CT (4) as shown by the arrows. (C) In contrast to mice receiving WT rice or PBS, mice orally vaccinated with rice-expressed CTB showed no symptoms of diarrhea and a low level of intestinal water. *, $P < 0.05$, CTB rice or rCTB vs. PBS.

serum of mice immunized with WT rice showed a massive elongation of CHO cells (Fig. 5*B*) similar to that induced by the native form of CT. Most important, when orally challenged with CT, the mice vaccinated with rice-expressed CTB showed no clinical sign of diarrhea (Fig. 5*C*), whereas those fed the WT rice or PBS developed severe diarrhea. However, some mice immunized with purified rCTB suffered from diarrhea (Fig. 5*C*). Consistent with these findings, the volume of intestinal water in mice immunized with rice-expressed CTB was significantly lower after challenge with CT than in mice receiving WT rice or PBS (Fig. 5*C*). These data directly demonstrate that oral vaccination with rice-expressed CTB could offer a high degree of protection against CT challenge.

Discussion

In this study, we have developed a physically and chemically stable and immunologically effective vaccine antigen-expressing transgenic rice seed that can withstand the harsh environment of the gastrointestinal tract and induce protective immunity against mucosal infections. The use of transgenic rice for vaccine production offers several benefits over other plants for vaccine production. For the implementation of global vaccination strategy, a well designed oral vaccine system should satisfy the following criteria: (*i*) produce sufficient quantities of inserted antigen for the immunization (33), (*ii*) preserve the expressed antigen for a long time at RT (9, 34), (*iii*) induce protective immunity (8, 34), (*iv*) protect from enzymatic digestion in gastrointestinal tract (8), and (*v*) effectively deliver the inserted antigen to mucosal inductive tissues, including antigen-sampling M cells (8, 35). Although several plants have currently been used for the creation of an "edible vaccine," seed crops such as soybean, maize, wheat, or rice seem to be the most suitable plants for fulfillment of the previous requirements. It was recently shown that a soybean-based oral vaccine expressing heat-labile toxin B subunit (LTB) of *E. coli* induced antigen-specific IgG and IgA responses (36). Although maize also has been used for the expression of LTB (20), a biological nature of long-distance pollen scattering is the major environmental concern (37). Further, the difficulty of transforming the inserted gene by use of the wheat vector system unfortunately disqualified its suitability for the oral vaccine development. In contrast, rice self-fertilizes, and thus its pollen is considered to fry within only 10 m (37). In addition, rice plants have unique features in the storage of protein using two systems of PB-I and PB-II (29), which are suitable for accumulation of vaccine antigen. Furthermore, rice is the only crop that full of genome sequences was elucidated, and thus it easily applied the genetic information for the creation of gene-manipulated product (38). It is expected that this 430-Mb genome information contributes to the development of useful transgenic rice (38).

To show the unique features and feasibility of rice-based mucosal vaccine, we purposely used CTB as a vaccine antigen because CTB has been immunologically well characterized and extensively used for the analysis of antigen-specific immune response in both mucosal and systemic compartments. One of the major limitations of plant-based vaccines is the achievement of a high expression of inserted vaccine antigen that is sufficient to induce protective immunity (33). To achieve high expression and accumulation of inserted vaccine antigen in rice seed, an endosperm-specific expression promoter gene, 2.3-kb *GluB-1*, followed by an endoplasmic reticulum retention signal peptide, KDEL, was used for the expression of CTB (Fig. 1*A*). By optimizing the codon usage of CTB for expression in rice, the accumulation level of CTB was achieved at ≈2.1% of total seed protein (0.15% of seed weight) (Fig. 1 *E* and *F*). Although CTB has been expressed in the potato, the level of expression was ≈0.3% of total protein (0.002% of fresh weight) in potato tubers (17); ≈4% of total leave protein (0.5% of leave weight) was achieved in tobacco leaves by using a chloroplast expression system (35). However, the tobacco leaf is not applicable in the practical sense for oral vaccination. Thus, the use of the rice transgenic system allowed the efficient expression of inserted vaccine antigen, although we cannot directly compare the level of the inserted antigen expression to other previously published plant-based vaccine systems.

The SDS/PAGE and Western blot analyses with anti-CTB polyclonal antibody showed two protein species with 12 kDa, which was almost the same as that of authentic CTB (39), and 15 kDa were detected (Fig. 1 *E* and *F*), suggesting that part of CTB expressed in rice seed might contain a full or partial *GluB-1* signal peptide at the N terminus. The SDS/PAGE under nonreducing conditions and subsequent Western blot analyses showed that the molecular mass of two protein species was shifted to 55–65 kDa (Fig. 1*F*). Because these two protein species were recognized by anti-CTB polyclonal antibody and possessed a molecular weight comparable to a pentameric structure under natural condition, most rice-expressed CTBs were considered to be a functionally native pentameric form for the induction of an antigen-specific immune response.

The tolerableness of inserted vaccine antigen in rice seed against the harsh digestive tract environment was also attributed by the site of protein accumulation in the rice seed. In general, rice starchy endosperm cells contain two types of protein storage organelles (PB-I and PB-II) with a different shape, density, and protein composition (29). PB-I and PB-II mainly contain prolamins (e.g., 13k prolamin) and glutelins (e.g., glutelin B1) as storage proteins, which are defined as alcohol- and water-soluble proteins, respectively (29, 30). Thus, glutelins (PB-II) are considered to be more digestible and sensitive than prolamins (PB-I) in the gastrointestinal tract. The immunoelectron microscopic analysis showed that CTB accumulation occurred in PB-I and PB-II of the endosperm cells of the rice seed (Fig. 2*A*). Thus, the direction of inserted protein expression (e.g., CTB) in PB-I seems to be responsible for the tract of resistance against digestive enzyme activity, and thus allows for

the effectiveness in the induction of antigen-specific immune response by minimum dose of oral antigen. To support this view, an *in vitro* pepsin digestion study showed that most of prolamin and ≈75% of the CTB accumulated in the rice seed were protected from the pepsin treatment, whereas most of the glutelin in the rice seed and all purified rCTB were digested (Fig. 2*B*). In contrast, LTB expressed in maize kernel seems to be less resistant to peptic degradation when compared to CTB in the rice seed because LTB protein was accumulated mainly in the starch granules of transgenic maize kernels (40). These finding indicated that accumulation of vaccine antigen in PB-I would provide physicochemical stability against digestive enzymatic effects. Taken together, the rice-based vaccine was stable and more effective than the purified subunit vaccine, as well as other plant-based vaccines, in the harsh environment of the gastrointestinal tract for the induction of protective immunity.

As described above, in the gastrointestinal tract, the antigens ingested from the luminal site are taken up by PPs via antigen-sampling cells known as M cells for initiation of antigen-specific T helper cells and IgA-committed B cells (41). Targeting vaccine antigen delivery to M cells should be a goal in mucosal vaccine development. Intestinal loop assay with rice-expressed CTB demonstrated that CTB were taken up by M cells (Fig. 3*A*). According to many biodegradable microsphere studies, the <10-μm microspheres have been shown to be efficient delivery vehicles into antigen-sampling M cells in PPs (42). The diameters of rice PB-I and PB-II range in size between 1 to 2 μm and 3 to 4 μm, respectively (43). In addition, PB-I, but not PB-II, accumulated most of its CTB at the surface, perhaps further enhancing antigen uptake by M cells. Taken together, these results demonstrated that rice-expressed CTBs were not only effectively taken up by M cells located in the follicle-associated epithelium of PPs, but also could serve as effective carriers of mucosal vaccines to intestinal inductive tissues such as the PPs.

Oral immunization with rice-expressed CTB induced CTB-specific serum IgG and mucosal IgA responses (Fig. 3*B*). A low dose of rice-expressed CTB (e.g., 50 mg of rice powder containing 75 μg CTB) sufficiently induced CTB-specific mucosal IgA responses, whereas the same contents of purified rCTB induced no or low levels of antigen-specific IgA responses (Fig. 3*B*). The differences in required dosage may be because of the physicochemical stability exhibited by rice-based mucosal vaccines and their ability to withstand digestive effects. Although oral immunization with rice-expressed CTB can induce CTB-specific immune responses, it did not induce any rice storage protein-specific immune responses (Fig. 3*C*), suggesting that rice-expressed CTB did not show adjuvant activity for rice protein. Furthermore, Southern blot analysis confirmed the genetic stability of the CTB-transgenic rice (data not shown); CTB expressed in the rice seed could be preserved for >1.5 years not only at 4°C, but also at RT, without any degradation (Fig. 4*A*), and the rice preserved for 1.5 years at RT induced an equal level of CTB-specific fecal IgA responses as freshly harvested rice (Fig. 4*B*). Our results provided further evidence for a significant potential benefit of rice-based mucosal vaccine for the development of stable vaccine with immunogenicity. Thus, a rice-based mucosal vaccine can be introduced as a first cold-chain-free vaccine.

Finally, we showed the protective effect induced by oral immunization with a rice-based mucosal vaccine. CT binds its receptor GM1-ganglioside, which is ubiquitously expressed in intestinal epithelium, and causes severe diarrhea (39). Our results demonstrated that the serum from mice immunized with rice-expressed CTB completely blocked the binding of CT to GM1-ganglioside (Fig. 5*A*) and also inhibited the elongation of CHO cells caused by CT (Fig. 5*B*). Most important, mice immunized with rice-expressed CTB showed no clinical sign of diarrhea after orally challenged with CT, whereas some mice immunized with purified rCTB suffered from diarrhea (Fig. 5*C*) perhaps because the level of antigen-specific mucosal IgA was lower in the purified rCTB-fed group than in the group receiving rice-expressed CTB. Therefore, we conclude that the rice-based mucosal vaccine would be effective for the induction of protective immunity compared to other types of mucosal vaccine.

In summary, we have developed a rice-based oral vaccine that offers significant advantages over currently available vaccines. In the rice-based vaccine, the vaccine antigen, CTB, accumulated in the PBs of starchy endosperm cells, from which they were taken up by M cells for the induction of antigen-specific mucosal immune responses with neutralizing activity. In addition, the rice-based CTB vaccine remained stable and maintained immunogenicity at RT for >1.5 years and was protected from pepsin digestion *in vitro*. Taken together, these findings suggest that a rice-based oral vaccine would be a most effective and highly practical vaccine regimen against infectious diseases, whether naturally occurring or stemming from acts of bioterrorism. Given its cost effectiveness and ease of administration, it would be a vaccine whose benefits could be fully enjoyed in developing countries, where the need is often the greatest.

Materials and Methods

DNA Constructions and Transformation of Rice Plants. The CTB gene of *V. cholerae* was modified to a suitable form for rice seed and inserted into a binary vector (pGPTV-35S-HPT) (23). The resulting plasmid (Fig. 1*A*) was transformed in two lines of rice plants, *Oryza sativa* L. cv Kitaake (24) and Hosetsu (25, 26), using an *Agrobacterium*-mediated method described previously (27).

DNA and RNA Analyses. Using the cetyltrimethylammonium bromide extraction method, we extracted genomic DNA from the leaf tissues of transgenic rice and analyzed the integration of the CTB gene in genomic DNA using PCR (23). The expression of mRNA encoding CTB in the rice seed was analyzed by Northern blot as previously described (23). Briefly, total RNA (30 μg) extracted from the developing seeds of rice plants using the phenol/chloroform extraction method was separated on a 1.0% (wt/vol) formaldehyde/agarose gel and transferred to Hybond N^+ membranes (GE Healthcare, Piscataway, NJ). The amplified CTB gene was used as a hybridization probe after labeling with [α-^{32}P] dCTP (GE Healthcare).

Protein Analyses. Total seed protein was extracted from seeds as described previously (23). Briefly, seeds of rice plants were ground to a fine powder using a Multibeads shocker (Yasui Kikai, Osaka, Japan) and extracted in 2% (wt/vol) SDS, 8 M urea, 5% (wt/vol) β-mercaptoethanol, 50 mM Tris·HCl (pH 6.8), and 20% (wt/vol) glycerol before being separated by SDS/PAGE with a 15% to 25% gradient polyacrylamide gel (Daiichi Pure Chemical, Tokyo, Japan). The gel was subsequently transferred to Hybond-P PVDF membranes (GE Healthcare) for Western blot analysis with 5 μg/ml rabbit anti-CTB antibody prepared in our laboratory. Accumulation levels of CTB were determined by densitometry analysis of Western blot against a standard curve generated with the use of rCTB expressed in *Bacillus brevis* and purified by using immobilized galactose (Pierce, Rockford, IL) in our laboratory (44). Using immunoelectron microscopic analysis, the distribution of CTB expressed in rice seed was analyzed. Briefly, rice seeds (at 12–15 days after flowering) were fixed with 4% paraformaldehyde (Wako, Osaka, Japan) and 0.1% glutaraldehyde (Nacalai Tesque, Kyoto, Japan) and embedded in LR White (London Resin, Hampshire, U.K.). Ultrathin sections (150 nm) were stained with 5 μg/ml rabbit anti-CTB antibody, followed by gold particle (20 nm)-conjugated goat anti-rabbit IgG (E.Y. Labs, San Mateo, CA) diluted to 1:10. The sections were then stained with 4% uranyl acetate and examined by using a transmission electron microscope (JEM100S; JEOL, Tokyo, Japan).

Pepsin Treatment. Seed powder (10 mg containing 15 μg of CTB) and purified rCTB (15 μg) were incubated with 0.5 mg/ml pepsin (2,500–3,500 units per mg protein; Sigma–Aldrich, St Louis, MO) in 0.1 ml of 0.1 M sodium acetate buffer (pH 1.7) with gentle rocking for 1 h at 37°C. After neutralization, the degradation of CTB, glutelin, or prolamin was analyzed by Western blot with 5 μg/ml rabbit anti-CTB, anti-glutelin GluB-1, or anti-13k prolamin antibodies prepared in our laboratory, respectively.

Uptake of CTB by M cells. A rice-expressed CTB or a nontransgenic rice was administered into an intestinal loop (≈1 cm) containing PPs of mice anesthetized by using 2 mg of ketamine (Sigma–Aldrich) per mouse. Thirty minutes after inoculation, the tissues were removed and fixed in tissue fixative (Genostaff, Tokyo, Japan) overnight at 4°C and then embedded in paraffin. Several mirror sections (5 μm) were subjected to immunohistochemistry with 5 μg/ml anti-CTB antibody and biotinylated anti-rabbit IgG (Vector Laboratories, Burlingame, CA) and to lectin histochemistry with 20 μg/ml biotinylated UEA-1 (Vector Laboratories). Both sections were finally incubated with SAB-PO (Nichirei, Tokyo, Japan) and visualized for the distribution of CTB and the localization of M cells by 3,3′-diaminobenzidine tetrahydrochloride (Dojin Laboratories, Kumamoto, Japan).

Oral Immunization. One immunization study was carried out by using 6-week-old C57BL/6J and BALB/c mice (CLEA, Tokyo, Japan). On six occasions at 2-week intervals, mice (six mice per group) were orally immunized with 12.5, 25, 50, or 100 mg of CTB-transgenic rice, with a corresponding dose of purified rCTB (18.75, 37.5, 75, or 150 μg) or with either 100 mg of nontransgenic rice dissolved in water or water alone as controls. For examination of the adjuvant effect of rice-expressed CTB, 100 mg of CTB-transgenic or WT rice was orally immunized with or without 10 μg of CT (List Biological Laboratories, Campbell, CA). One week after the final immunization, serum and fecal extracts were collected, and CTB or rice storage protein-specific Ig responses were measured by ELISA with 5 μg/ml rCTB or 20 μg/ml rice-storage protein extracted with 0.01% Triton X-100 as described previously (45).

Neutralizing Assay. Serial-diluted serum collected from immunized mice were treated with 50 ng/ml of CT and subjected to GM1-ELISA as previously described with some modifications (17). Briefly, 5 μg/ml of monosialoganglioside GM1 (Sigma–Aldrich)-coated 96-well plates (Thermo, Milford, MA) were incubated with CT that had been treated first with serum from immunized mice and then with an HRP-conjugated anti-CTB antibody prepared in our laboratory. The color was developed with the addition of TMB substrate (Moss, Pasadena, MD), and absorbance was measured at 450 nm. In addition, a CHO cell (ATCC, CCL-61) assay (32) was performed by using serum treated with 50 ng/ml CT. After 14 h of stimulation in 5% CO_2 in a humidified incubator at 37°C, morphological changes were observed under a microscope. In addition, we performed an *in vivo* challenge experiment with CT. The vaccinated mice were orally challenged with 20 μg of CT. After 14 h, clinical symptoms of diarrhea were observed, and the volume of intestinal water was measured.

Data Analysis. Data are expressed as the mean ± SD. All analyses for statistically significant differences were performed with Tukey's *t* test, with *P* values of <0.01 and <0.05 considered significant.

We thank Drs. Kimberly McGhee and Prosper N. Boyaka for critically reading and editing the manuscript and Nippon Paper Group, Inc., and Rohto Pharmaceutical Co., Ltd., for contributions. This work was supported by the Core Research for Evolutional Science and Technology program (H.K.); the Creation and Support Program for Start-Ups for Universities (Y.Y.) from the Japan Science and Technology Corporation; a grant-in-aid from the Ministry of Education, Culture, Sports, Science, and Technology and the Ministry and Health and Labor (H.K.); the Development of Fundamental Technologies for Production of High-Value Materials Using Transgenic Plants project from the Ministry of Economy, Trade, and Industry (H.K.); and the Functional Analysis of Genes Relevant to Agriculturally Important Traits in Rice Genome project from the Ministry of Agriculture, Forestry, and Fisheries (F.T.).

1. Watanabe I, Hagiwara Y, Kadowaki SE, Yoshikawa T, Komase K, Aizawa C, Kiyono H, Takeda Y, McGhee JR, Chiba J, *et al.* (2002) *Vaccine* 20:3443–3455.
2. Bukreyev A, Lamirande EW, Buchholz UJ, Vogel LN, Elkins WR, St Claire M, Murphy BR, Subbarao K, Collins PL (2004) *Lancet* 363:2122–2127.
3. Belyakov IM, Hel Z, Kelsall B, Kuznetsov VA, Ahlers JD, Nacsa J, Watkins DI, Allen TM, Sette A, Altman J, *et al.* (2001) *Nat Med* 7:1320–1326.
4. Czerkinsky C, Anjuere F, McGhee JR, George-Chandy A, Holmgren J, Kieny MP, Fujiyashi K, Mestecky JF, Pierrefite-Carle V, Rask C, Sun JB (1999) *Immunol Rev* 170:197–222.
5. Kiyono H, Fukuyama S (2004) *Nat Rev Immunol* 4:699–710.
6. Holmgren J, Czerkinsky C (2005) *Nat Med* 11:S45–S53.
7. Neutra MR, Kozlowski PA (2006) *Nat Rev Immunol* 6:148–158.
8. Yuki Y, Kiyono H (2003) *Rev Med Virol* 13:293–310.
9. Varmus H, Klausner R, Zerhouni E, Acharya T, Daar AS, Singer PA (2003) *Science* 302:398–399.
10. Giudice EL, Campbell JD (2006) *Adv Drug Deliv Rev* 58:68–89.
11. Varmus H, Klausner R, Zerhouni E, Acharya T, Daar AS, Singer PA (2003) *Science* 302:398–399.
12. Streatfield SJ, Howard JA (2003) *Int J Parasitol* 33:479–493.
13. Curtiss R1, Cardineau CA (1997) US Patent 5,686,079.
14. Haq TA, Mason HS, Clements JD, Arntzen CJ (1995) *Science* 268:714–716.
15. Mason HS, Ball JM, Shi JJ, Jiang X, Estes MK, Arntzen CJ (1996) *Proc Natl Acad Sci USA* 93:5335–5340.
16. Tacket CO, Mason HS, Losonsky G, Clements JD, Levine MM, Arntzen CJ (1998) *Nat Med* 4:607–609.
17. Arakawa T, Chong DK, Langridge WH (1998) *Nat Biotechnol* 16:292–297.
18. Richter LJ, Thanavala Y, Arntzen CJ, Mason HS (2000) *Nat Biotechnol* 18:1167–1171.
19. Sandhu JS, Krasnyanski SF, Domier LL, Korban SS, Osadjan MD, Buetow DE (2000) *Transgenic Res* 9:127–135.
20. Streatfield SJ, Jilka JM, Hood EE, Turner DD, Bailey MR, Mayor JM, Woodard SL, Beifuss KK, Horn ME, Delaney DE, *et al.* (2001) *Vaccine* 19:2742–2748.
21. Mason HS, Haq TA, Clements JD, Arntzen CJ (1998) *Vaccine* 16:1336–1343.
22. Walmsley AM, Arntzen CJ (2003) *Curr Opin Biotechnol* 14:145–150.
23. Takagi H, Hiroi T, Yang L, Tada Y, Yuki Y, Takamura K, Ishimitsu R, Kawauchi H, Kiyono H, Takaiwa F (2005) *Proc Natl Acad Sci USA* 102:17525–17530.
24. Goto F, Yoshihara T, Shigemoto N, Toki S, Takaiwa F (1999) *Nat Biotechnol* 17:282–286.
25. Hedden P (2003) *Nat Biotechnol* 21:873–874.
26. Kurita A, Itoh M, Takenaka S, Makino H, Morita S, Masumura T, Tanaka K (2002) *Plant Biotechnol* 19:81–85.
27. Hiei Y, Ohta S, Komari T, Kumashiro T (1994) *Plant J* 6:271–282.
28. Frey A, Giannasca KT, Weltzin R, Giannasca PJ, Reggio H, Lencer WI, Neutra MR (1996) *J Exp Med* 184:1045–1059.
29. Yamagata H, Tanaka K (1986) *Plant Cell Physiol* 27:135–145.
30. Katsube T, Kurisaka N, Ogawa M, Maruyama N, Ohtsuka R, Utsumi S, Takaiwa F (1999) *Plant Physiol* 120:1063–1074.
31. Sharma R, Schumacher U, Adam E (1998) *J Histochem Cytochem* 46:143–148.
32. Kothary MH, Claverie EF, Miliotis MD, Madden JM, Richardson SH (1995) *Infect Immun* 63:2418–2423.
33. Chargelegue D, Obregon P, Drake PM (2001) *Trends Plants Sci* 6:495–496.
34. Levine MM, Sztein MB (2004) *Nat Immunol* 5:460–464.
35. Daniell H, Lee SB, Panchal T, Wiebe PO (2001) *J Mol Biol* 311:1001–1009.
36. Moravec T, Schmidt MA, Herman EM, Woodford-Thomas T (2007) *Vaccine* 25:1647–1657.
37. Abe Y, Shimizu N, Okawa K (1978) *Res Bull Aichi Agric Res Centr* A10:37–43.
38. Sasaki T, Matsumoto T, Yamamoto K, Sakata K, Baba T, Katayose Y, Wu J, Niimura Y, Cheng Z, Nagamura Y, *et al.* (2002) *Nature* 420:312–316.
39. Mekalanos JJ, Swartz DJ, Pearson GD, Harford N, Groyne F, de Wilde M (1983) *Nature* 306:551–557.
40. Chikwamba RK, Scott MP, Mejia LB, Mason HS, Wang K (2003) *Proc Natl Acad Sci USA* 100:11127–11132.
41. Owen RL (1977) *Gastroenterology* 72:440–451.
42. Mestecky J, Blumberg RS, Kiyono H, McGhee JR (2003) in *Fundamental Immunology*, ed Paul WE (Lippincott Williams & Wilkins, Philadelphia), 5th Ed, pp 965–1020.
43. Yamagata H, Sugimoto T, Tanaka K, Kasai Z (1982) *Plant Physiol* 70:1094–1100.
44. Yuki Y, Byun Y, Fujita M, Izutani W, Suzuki T, Udaka S, Fujihashi K, McGhee JR, Kiyono H (2001) *Biotechnol Bioeng* 74:62–69.
45. Yamamoto M, Kweon MN, Rennert PD, Hiroi T, Fujihashi K, McGhee JR, Kiyono H (2004) *J Immunol* 173:762–769.

Functional B7.2 and B7-H2 Molecules on Myeloma Cells Are Associated with a Growth Advantage

Taishi Yamashita,[1,3] Hideto Tamura,[1] Chikako Satoh,[1,4] Eiji Shinya,[2] Hidemi Takahashi,[2] Lieping Chen,[5] Asaka Kondo,[1] Takashi Tsuji,[3] Kazuo Dan,[1] and Kiyoyuki Ogata[1]

Abstract

Purpose: B7 family molecules expressed on antigen-presenting cells stimulate or inhibit normal immune responses. The aim of this study was to investigate whether functional B7.2 and B7-H2 molecules are expressed on myeloma cells and, if so, whether they are associated with pathophysiology in myeloma.

Experimental Design: The expression of B7.2 and B7-H2 molecules on normal plasma and neoplastic (myeloma) plasma cells was analyzed. The cell proliferation and immunomodulatory function of myeloma cells related to B7.2 and B7-H2 expression were examined.

Results: Human myeloma cell lines commonly expressed B7.2 and B7-H2 molecules. B7.2 expression on plasma cells was more common in myeloma patients ($n = 35$) compared with that in patients with monoclonal gammopathy of unknown significance ($n = 12$) or hematologically normal individuals ($n = 10$). Plasma cells expressing B7-H2 were observed in myeloma patients alone, although rarely. Patients whose myeloma cells showed high B7.2 expression were more anemic and thrombocytopenic than other myeloma patients. The expression of these molecules was induced or augmented by cultivating myeloma cells with autologous stroma cells or tumor necrosis factor-α, a key cytokine in myeloma biology. Cell proliferation was more rapid in the $B7.2^+$ and $B7\text{-}H2^+$ populations compared with the $B7.2^-$ and $B7\text{-}H2^-$ populations, respectively, in the human myeloma cell lines examined. B7.2 and B7-H2 molecules on myeloma cells induced normal $CD4^+$ T cells to proliferate and produce soluble factors, including interleukin-10 that stimulate myeloma cell proliferation.

Conclusions: Functional B7.2 and B7-H2 molecules detected on myeloma cells may be involved in the pathophysiology of myeloma.

Multiple myeloma (MM) is a virtually incurable hematologic malignancy characterized by monoclonal growth of plasma cells (myeloma cells). In addition to the well-known deficiency in B-cell immunity, T-cell dysfunction, such as reduced cytotoxic activity (1) and reduced responsiveness to interleukin 2 (IL-2; refs. 2, 3), has been reported, which may weaken antitumor immune responses in MM patients. The interaction between myeloma cells and bone marrow (BM) stroma cells stimulates the production of a variety of cytokines that are involved in the pathophysiology of MM (4, 5). Those include IL-6, IL-10, and tumor necrosis factor-α (TNF-α), which stimulate myeloma cell growth (6–9). An interesting aspect is that both IL-10 and TNF-α have an immunomodulating function, including inhibition of CTLs (10–12).

The B7 family molecules play an important role in the immune response by costimulating or coinhibiting T cells via antigen–T-cell receptor interactions (13–16). Interactions between B7.1/B7.2 ligands on professional antigen-presenting cells and CD28/CTLA-4 receptors on T cells represent a classic pathway and control antigen-specific T-cell proliferation, anergy, and survival. B7-H2 is another B7 family molecule induced by TNF-α (17). The binding of B7-H2 to the inducible costimulatory receptor (ICOS), a counterreceptor, induces T cells to proliferate and secrete both Th1 and Th2 cytokines, such as IFN-γ and IL-4 but not the potent Th1 cytokine IL-2 (18). Furthermore, the B7-H2-ICOS signal induces IL-10 production, which plays an important role in reducing immune responses (19, 20). B7 family molecules are expressed not only on professional antigen-presenting cells but also on some tumor cells and the latter may modulate antitumor immunity in hosts. For example, we detected the expression of B7.2 and B7-H2 molecules on blasts from patients with acute myeloid leukemia and showed that these molecules on acute myeloid

Authors' Affiliations: [1]Division of Hematology, Department of Medicine and [2]Department of Microbiology and Immunology, Nippon Medical School, Tokyo, Japan; [3]Department of Biological Science and Technology, Tokyo University of Science, Chiba, Japan; [4]Department of Bioregulation, Institute of Development and Aging Science, Nippon Medical School, Kawasaki, Japan; and [5]Department of Dermatology, Department of Oncology and Institute for Cell Engineering, Johns Hopkins University School of Medicine, Baltimore, Maryland

Received 2/24/08; revised 10/21/08; accepted 10/25/08.

Grant support: A Grant-in-Aid for Scientific Research from the Japan Society for the Promotion of Science (no. 20591157).

The costs of publication of this article were defrayed in part by the payment of page charges. This article must therefore be hereby marked *advertisement* in accordance with 18 U.S.C. Section 1734 solely to indicate this fact.

Note: Supplementary data for this article are available at Clinical Cancer Research Online (http://clincancerres.aacrjournals.org/).

Requests for reprints: Hideto Tamura, Division of Hematology, Department of Medicine, Nippon Medical School, 1-1-5 Sendagi, Bunkyo-ku, Tokyo 113-8603, Japan. Phone: 81-3-3822-2131; Fax: 81-3-5685-1793; E-mail: tam@nms.ac.jp.

doi:10.1158/1078-0432.CCR-08-0501

Translational Relevance

Multiple myeloma (MM) is a virtually incurable hematologic malignancy. Therefore, research that could result in improved MM treatment and/or a breakthrough in our understanding of this disease is very important. This article shows that myeloma cells from a substantial number of MM patients express functional B7.2 or B7-H2 molecules. Furthermore, it provides evidence that these molecules on myeloma cells may be involved in the pathophysiology of the disease. It is anticipated that these data will be translated into a new therapeutic strategy for MM.

leukemia blasts inhibited anti-acute myeloid leukemia immunity *in vitro* and were associated with poor patient prognosis (21). In MM, data on B7 family molecules are lacking. To the best of our knowledge, only one study examined this topic. Pope et al. (22) observed that MM patients whose tumor cells expressed B7.2 molecules had a poor prognosis. However, they did not examine whether the B7.2 molecules on myeloma cells were functional. Here, we investigated whether functional B7.2 and B7-H2 molecules are expressed on myeloma cells and, if so, whether these B7 molecules are associated with pathophysiology in MM.

Materials and Methods

Cell lines. Eleven human myeloma cell lines (HMCL), KMM-1, KMS-11, KMS-12BM, KMS-12PE, KMS-18, KMS-20, KMS-26, KMS-27, KMS-28BM, KMS-28PE, and KMS-34, were kindly provided by Dr. Otsuki (Kawasaki Medical School, Okayama, Japan). PCM6 cells were obtained from the Riken Cell Bank, and RPMI8226 and U266 cells were from the American Type Culture Collection. PCM6 cells were maintained in McCoy's 5A modified medium (Life Technologies) containing 20% FCS and 3 ng/mL of recombinant IL-6 (Kirin Brewery Co.). The other cells were maintained in complete medium, i.e., RPMI 1640 supplemented with 10% FCS and 2 mmol/L L-glutamine. In experiments examining the effects of cytokines on these cells, TNF-α

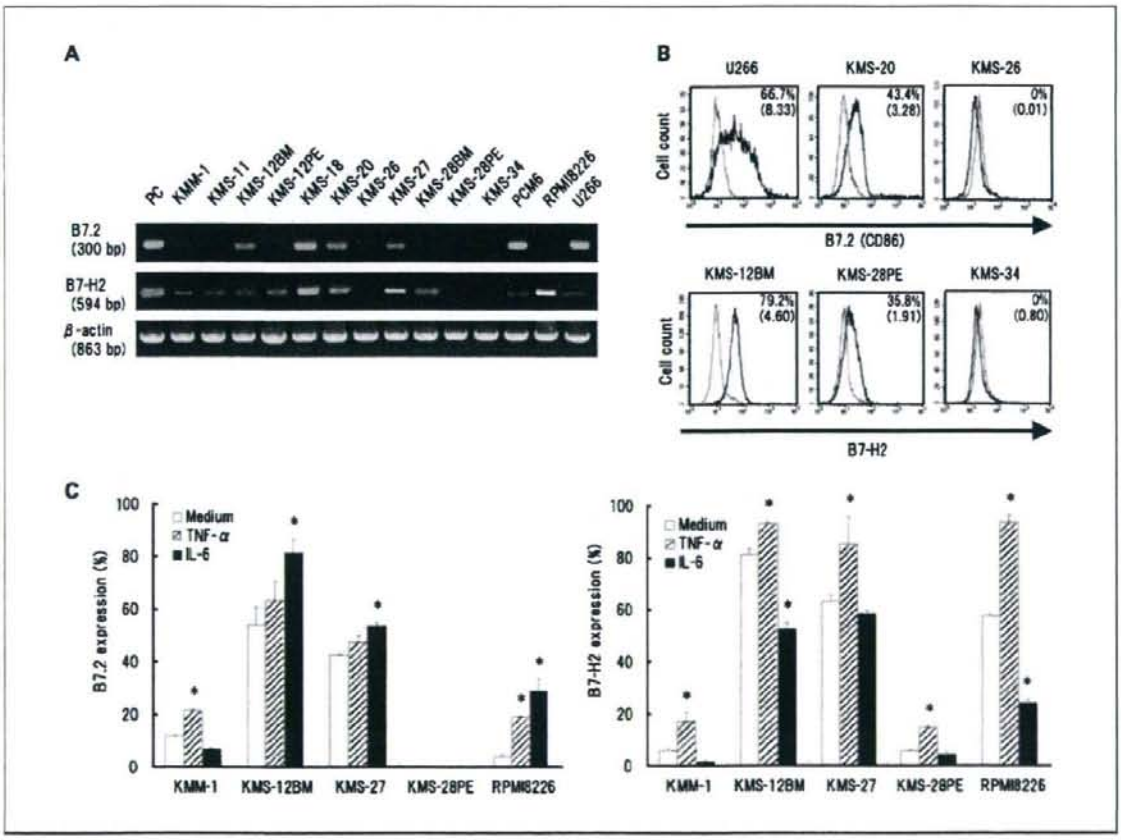

Fig. 1. *A*, B7.2 and B7-H2 mRNA expression analyzed using reverse transcription-PCR in 14 HMCLs. Equal amounts of cDNA from each cell line were amplified using primers specific for B7.2, B7-H2, and β-actin. *B*, representative flow cytometry analyses of the B7.2 and B7-H2 expression in HMCLs. Bold curves, staining with anti-B7.2 or anti-B7-H2 mAb; thin curves, staining with isotype-matched control immunoglobulin. Data are expressed in the percentages of positive cells and in relative mean fluorescence intensity (*numbers in parentheses*). *C*, effects of TNF-α and IL-6 on B7.2 and B7-H2 expression in HMCLs. Columns, mean of three independent experiments; bars, SD. Medium, no cytokine was added. *, $P < 0.05$, significantly different from Medium.

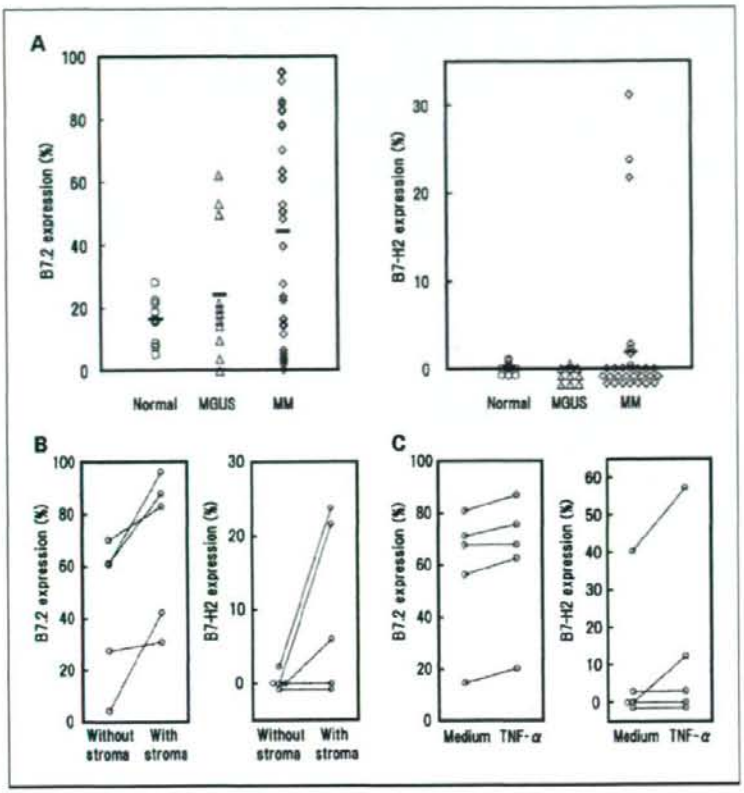

Fig. 2. *A*, percentages of B7.2$^+$ and B7-H2$^+$ plasma cells among all plasma cells in 10 hematologically normal individuals and 12 monoclonal gammopathy of unknown significance and 35 MM patients determined using flow cytometry. Horizontal bars, mean. Effects of autologous stroma cells (*B*) and TNF-α (*C*) on B7.2 and B7-H2 expression on myeloma cells from patients.

(500 units/mL; PeproTech), IL-10 (10 ng/mL; MBL), or IL-6 (10 ng/mL) were added to the cultures. The cell number was counted using the trypan blue dye-exclusion method.

In some experiments, B7.2$^+$, B7.2$^-$, B7-H2$^+$, or B7-H2$^-$ KMS-27 cells were purified with FACSVantage (Becton Dickinson) as described previously (23).

Patients, hematologically normal individuals, and cell preparation. BM samples were obtained from individuals who underwent BM aspiration for diagnostic purposes after obtaining written informed consent. They included 35 MM patients [4 stage I and 31 stage III according to the definition of Durie and Salmon (24)], 12 patients with monoclonal gammopathy of unknown significance, and 10 hematologically normal individuals. All BM samples from MM patients were obtained at the initial diagnosis, except for those from 6 patients, 2 of whose samples showed that they were refractory to conventional chemotherapy and 4 of whose samples were in the plateau phase according to the standard definition. Diagnoses were made according to the WHO classification. Mononuclear cells were separated from BM samples with Histopaque (Sigma) density centrifugation. These cells were used immediately or cryopreserved in liquid nitrogen until use. In cell samples from hematologically normal individuals, CD19-positive cells were enriched from BM mononuclear cells using magnetic cell sorting (Miltenyi Biotec; ref. 23) to ensure plasma cell identification in flow cytometry (25). This study was approved by the institutional review board of Nippon Medical School.

Stroma cells were prepared as follows. BM mononuclear cells from MM patients (2×10^6/mL) were plated in 6-well plates in complete medium. The cultures were fed weekly by removing 75% of the medium and adding fresh medium to make up the same volume. After the cultivated cells became adherent, stromal cell shaped, positive for mesenchymal stem cell markers (CD44 and CD90), and negative for hematopoietic markers (CD34, CD45, and CD11b), they were used as stroma cells (26). In experiments inducing B7.2 and B7-H2 expression, mononuclear cells were cultured in complete medium on autologous stroma cells for 3 wk or with TNF-α (500 units/mL) for 2 d.

Reverse transcription-PCR. Total RNA extracted from each HMCL was reverse transcribed with Superscript II Reverse transcriptase (Invitrogen) using random hexamers. PCR amplification was done using the primer sets for B7.2 and B7-H2 and PCR conditions previously described (21).

Flow cytometry. Immunophenotyping was done with FACScan (Becton Dickinson; refs. 21, 27). Briefly, after blocking with human immunoglobulin, patient BM samples were stained with anti-CD38 monoclonal antibody (mAb) labeled with FITC and phycoerythrin-labeled anti-B7.2 (Becton Dickinson) or anti-B7-H2 mAb (e-Bioscience). Plasma cells were identified by a high expression of CD38 molecules (22). We also confirmed that the identified plasma cells expressed another plasma cell marker, CD138 (Becton Dickinson). Examples of flow cytometry analysis are shown in Supplementary Fig. S1. HMCLs were single stained with FITC/phycoerythrin-conjugated mAbs against lymphocyte function-associated antigen-1 (LFA-1), intercellular adhesion molecule-1 (ICAM-1; Beckman Coulter), very late antigen-4, vascular cell adhesion molecule-1 (Becton Dickinson), B7.2, and B7-H2.

Cell cycle analysis. After blocking with human immunoglobulin, HMCLs were stained with purified mouse anti-B7.2 or anti-B7-H2

mAbs. The cells were washed and further incubated with FITC-conjugated antimouse IgG (Biosource). Then, the cells were fixed with 70% ethanol at 4°C for 3 h. The fixed cells were washed and resuspended in 100 μL of PBS and 1 μg of RNase (Qiagen) containing 0.1 mg/mL of propidium iodide (Sigma). The cell cycle profiles of B7.2$^+$, B7.2$^-$, B7-H2$^+$, and B7-H2$^-$ HMCLs were analyzed using flow cytometry.

Colony-forming assay. Purified B7.2$^+$, B7.2$^-$, B7-H2$^+$, and B7-H2$^-$ cells (1×10^3 per culture dish) were cultured in MethoCult H4230 methylcellulose medium (StemCell Technologies; ref. 23). Colonies (aggregates of 50 or more cells) were scored on day 14 of culture.

Mixed lymphocyte-myeloma reaction. CD4$^+$ T cells (purity > 95%) were prepared from peripheral blood of healthy volunteers on magnetic cell sorting columns (21). These cells (1×10^5) were cocultured with irradiated (20,000 rad) myeloma cells (1×10^5) expressing both B7.2 and B7-H2 molecules in microtiter wells for 5 d. Antagonistic mAbs (10 μg/mL) against B7.2 and ICOS (e-Bioscience) were added to the cultures to block the B7.2-CD28 and B7-H2-ICOS pathways, respectively. During the final 18 h of culture, [^{3}H]thymidine (1 μCi/well) was added to determine T-cell proliferation. All samples were assayed at least in quadruplicate.

In some experiments, culture supernatants of mixed lymphocyte-myeloma reaction (MLMR) were collected on day 5 of culture. The

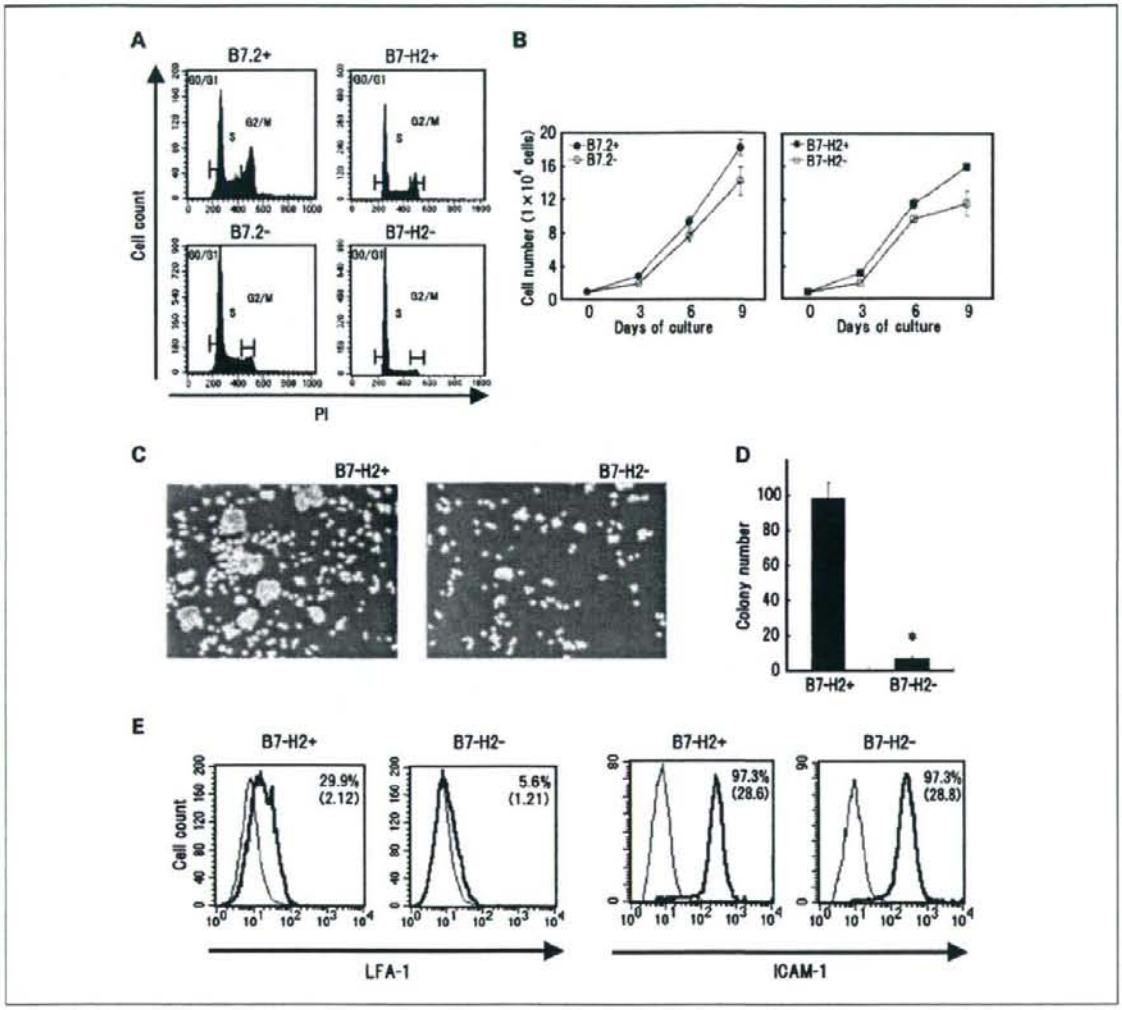

Fig. 3. *A*, cell cycle analyses of B7.2$^+$ or B7.2$^-$ KMS-27 cells (*left*) and of B7-H2$^+$ or B7-H2$^-$ KMS-27 cells (*right*). Each cell population was gated and analyzed in flow cytometry. Analysis on at least 10,000 events for each sample. The cell cycle data were reproducible when B7-H2$^+$ and B7-H2$^-$ KMS-27 cells isolated using FACSVantage were analyzed (data not shown). *B*, proliferation of isolated B7.2$^+$ or B7.2$^-$ KMS-27 cells and B7-H2$^+$ or B7-H2$^-$ KMS-27 cells. Points, mean of three independent experiments; bars, SD. *C*, photomicrographs of purified B7-H2$^+$ and B7-H2$^-$ KMS-27 cells during exponential cell growth in culture. *D*, number of colonies (defined as aggregates composed of 20 or more cells) formed by purified B7-H2$^+$ and B7-H2$^-$ cells on day 7 of culture. Columns, mean of three independent triplicate cultures; bars, SD. *, $P < 0.01$ compared with the data of B7-H2$^+$. *E*, representative flow cytometry analyses of LFA-1 and ICAM-1 expression on B7-H2$^+$ and B7-H2$^-$ KMS-27 cells. Bold curves, staining with anti – LFA-1 or anti – ICAM-1 mAb; thin curves, staining with isotype-matched control immunoglobulin. Data are expressed in percentages of positive cells and in relative mean fluorescence intensity (*numbers in parentheses*).

concentrations of IFN-γ, IL-2, IL-4, and IL-10 in the supernatants were measured with sandwich ELISA kits (eBioscience).

Coculture using a transwell system. KMS-27 (1×10^4) cells were plated onto a transwell membrane insert (Nunc) placed above the culture containing normal $CD4^+$ T cells (1×10^5) with or without irradiated KMS-27 cells (1×10^5). Antihuman IL-10 polyclonal antibody (R&D Systems), anti-B7.2, and/or anti-ICOS mAbs were added to the lower cultures to neutralize their biological activities. After 5 d of culture, KMS-27 cells above the insert were harvested and counted using the trypan blue dye-exclusion method.

Statistical analysis. Differences between two groups of data were determined with the χ^2 test and Student's t test for categorical and continuous variables, respectively, unless otherwise stated. The Mann-Whitney U test was used for two groups of data with continuous nonparametric variables. A P value of <0.05 was considered significant.

Results

Expression and induction of B7.2 and B7-H2 molecules on HMCLs. First, we analyzed the expression of B7.2 and B7-H2 molecules on HMCLs. Seven and 11 of 14 HMCLs expressed high levels of B7.2 and B7-H2 mRNA, respectively (Fig. 1A). These results were consistent with the protein expression analyzed using flow cytometry (Fig. 1B; Supplementary Table S1): The expression of B7.2 and B7-H2 molecules was detected in 7 (50.0%) and 9 (64.3%) HMCLs, respectively. Next, we examined whether cytokines, i.e., TNF-α, IL-6, or IL-10, affect B7.2 and B7-H2 expression in five HMCLs. TNF-α up-regulated the expression of both molecules in almost all cell lines examined. Meanwhile, IL-6 up-regulated B7.2 expression in three of five HMCLs and down-regulated B7-H2 expression in two of five HMCLs (Fig. 1C). IL-10 did not affect the expression of these molecules (data not shown).

Expression and induction of B7.2 and B7-H2 molecules in myeloma patients. Using flow cytometry, we examined the expression of B7.2 and B7-H2 molecules on fresh plasma cells. The percentages of $B7.2^+$ cells in plasma cells were much higher in MM patients than those in monoclonal gammopathy of unknown significance patients or in hematologically normal individuals (Fig. 2A, *left*; MM versus monoclonal gammopathy of unknown significance, $P = 0.0318$; MM versus normals, $P = 0.0145$; Mann-Whitney U test). When MM patients were divided into two groups using various cutoff percentages of B7.2 positivity, those in whom >40% of myeloma cells expressed B7.2 ($n = 18$, called $B7.2^{high+}$ MM patients in this article) showed significantly lower levels of hemoglobin and platelets compared with other MM patients ($B7.2^{-/low}$ MM patients in this article, $n = 17$; Supplementary Table S2). Although there was no difference in survival between the two groups of patients (data not shown), both patients refractory to chemotherapy were in the $B7.2^{high+}$ group and all four patients in the plateau phase were in the $B7.2^{-/low}$ group. Meanwhile, B7-H2 expression on plasma cells was clearly documented only in three MM patients. The disease of these three patients was intractable: one patient had plasma cell leukemia and the other two had chemotherapy-resistant MM. In our cohort of patients, BM cells from only two MM patients were analyzed for B7.2 and B7-H2 expression in different disease statuses at the initial diagnosis and at the stage of refractory disease. The expression of these molecules on myeloma cells was augmented at the refractory stage in both patients, except for B7-H2 expression in one patient in whom B7-H2 was not detected at either time point (Supplementary Table S3). All of the above findings support the idea that these molecules may be associated with disease progression in MM, although the clinical evidence remains insufficient for the B7-H2 molecule because of the rarity of B7-H2–positive patients.

Next, we examined whether stroma cells and TNF-α, both important for myeloma cell proliferation *in vivo*, modulate the expression of B7.2 and B7-H2 on myeloma cells from MM patients. B7.2 or B7-H2 expression on myeloma cells from >50% of patients examined was up-regulated after the cells were cultivated with autologous stroma cells or TNF-α (Fig. 2B and C).

Cell cycle and proliferation of myeloma cells based on B7.2 and B7-H2 expression. Based on the above data, we speculated that B7.2 or B7-H2 expression on myeloma cells was associated with their proliferative potential. When KMS-27 cells that did or did not express these B7 family molecules were analyzed, $B7.2^+$ and $B7\text{-}H2^+$ cells had significantly fewer G_0-G_1 phase cells and more G_2-M phase cells compared with $B7.2^-$ and $B7\text{-}H2^-$ cells, respectively (Fig. 3A; Table 1). Consistent with these results, the $B7.2^+$ and $B7\text{-}H2^+$ KMS-27 cells proliferated more rapidly in liquid cultures and formed more colonies in semisolid cultures compared with the $B7.2^-$ and $B7\text{-}H2^-$ KMS-27 cells, respectively (Fig. 3B; Supplementary Table S4). The same growth advantage of myeloma cells expressing B7.2 and B7-H2 molecules was also documented in all other HMCLs examined (Table 1; Supplementary Table S4; Supplementary Fig. S2).

We then examined whether myeloma cells have a growth advantage when the cells are induced to express B7.2 and B7-H2 molecules. When RPMI8226 cells, for which B7.2 and B7-H2 expression is inducible by TNF-α as shown in Fig. 1C, were treated with TNF-α, the cell cycle of the cells was clearly

Table 1. Cell cycling of HMCLs as a function of B7.2 and B7-H2 expression

Cell fraction in HMCLs	Cell cycle		
	G_0-G_1	S	G_2-M
KMS-27 cells			
$B7.2^+$	52.8 ± 0.9*	19.7 ± 0.1	27.6 ± 0.9*
$B7.2^-$	80.8 ± 1.6	16.0 ± 1.5	3.7 ± 0.4
$B7\text{-}H2^+$	53.7 ± 1.4*	18.6 ± 2.2	28.0 ± 0.9*
$B7\text{-}H2^-$	78.5 ± 0.8	17.5 ± 0.8	4.1 ± 1.3
KMS-20 cells			
$B7.2^+$	42.5 ± 0.7*	20.0 ± 0.1*	37.7 ± 0.8*
$B7.2^-$	74.2 ± 1.0	13.7 ± 0.6	12.3 ± 0.3
$B7\text{-}H2^+$	43.4 ± 1.1*	26.9 ± 0.4*	30.2 ± 0.6*
$B7\text{-}H2^-$	81.5 ± 0.9	13.4 ± 0.7	4.8 ± 0.3
U266 cells			
$B7.2^+$	49.5 ± 4.0*	23.7 ± 1.6	25.7 ± 3.8*
$B7.2^-$	65.0 ± 2.7	21.2 ± 0.5	13.9 ± 1.7
RPMI8226 cells			
$B7\text{-}H2^+$	39.5 ± 0.9*	33.1 ± 2.2*	26.9 ± 4.1*
$B7\text{-}H2^-$	64.4 ± 3.0	25.8 ± 2.4	9.3 ± 2.1

NOTE: Mean ± SD of three independent experiments. $B7\text{-}H2^+$ and $B7.2^+$ fractions in U266 and RPMI8226 cells, respectively, were sparse and thus were not analyzed.
*Significant difference ($P < 0.05$) when data of each cell cycle phase were compared between $B7.2^+$ (or $B7\text{-}H2^+$) and $B7.2^-$ (or $B7\text{-}H2^-$) cell fractions in each HMCL.

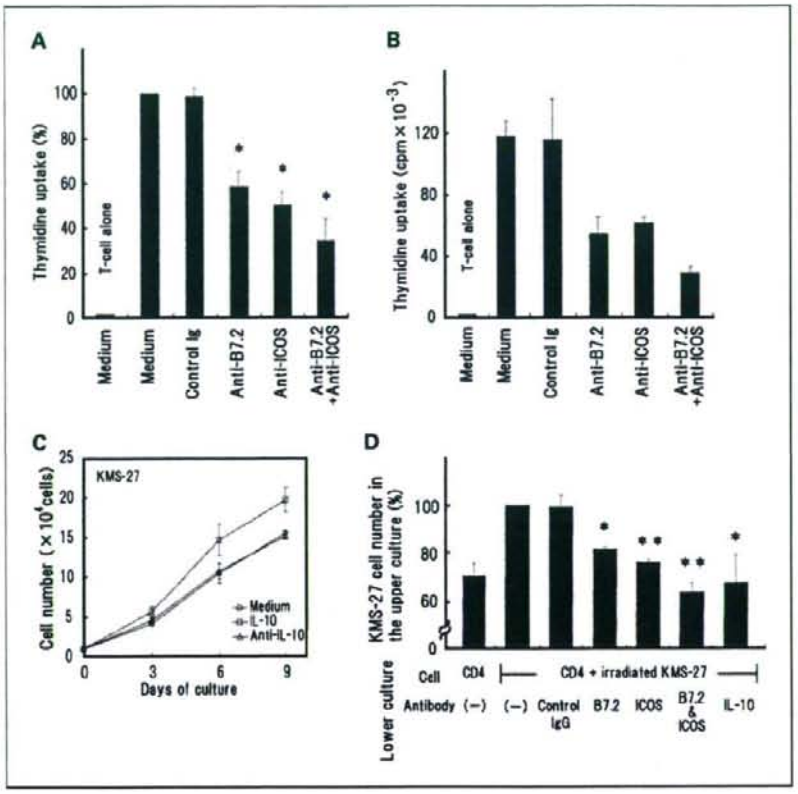

Fig. 4. *A*, MLMR. Normal CD4⁺ Tcells were cultured with (*five columns, right*) or without (*first column, left*) irradiated KMS-27 cells that expressed B7.2 and B7-H2. Effects of anti-B7.2 and anti-ICOS blocking mAbs on CD4⁺ T-cell proliferation were examined in this assay. Columns, mean of three independent triplicate cultures, in which the second column from the left was defined as 100%; bars, SD. Medium, no antibody was added. *, $P < 0.01$ compared with the data for control immunoglobulin. *B*, MLMR done using the same method as described in *A*, except that irradiated patient MM cells expressing B7.2 and B7-H2 were used instead of KMS-27 cells. Columns, mean of triplicate cultures; bars, SD. *C*, kinetics of KMS-27 cell proliferation. The cells were cultured in medium alone or in medium containing anti–IL-10 neutralizing antibody or recombinant IL-10. Points, mean of three independent experiments; bars, SD. *D*, cultures using a transwell system. KMS-27 cells were plated onto a transwell membrane insert, which was placed above the culture containing CD4⁺ Tcells alone (*first columns, left*) or CD4⁺ Tcells with irradiated KMS-27 cells (*six columns, right*). Blocking antibodies to B7.2, ICOS, and/or IL-10 were added to the lower cultures and their effects on KMS-27 cell proliferation in the upper cultures were examined. Columns, mean of three independent triplicate cultures, in which the second column from the left was defined as 100%; bars, SD. *, $P < 0.05$; **, $P < 0.01$ compared with the data for control immunoglobulin.

stimulated (Supplementary Table S5). Furthermore, when 293T cells (a human kidney cell line suitable for efficient transfection experiments) were transfected with either B7.2 or B7-H2 gene or Mock, B7.2 or B7-H2 gene induction induced cell cycle activation (Supplementary Table S6).

We noted that even in liquid culture, B7-H2⁺ KMS-27 cells often formed colonies during exponential cell growth (Fig. 3C): There were many more colonies of B7-H2⁺ cells compared with B7-H2⁻ cells in liquid culture (Fig. 3D). Meanwhile, there was no difference in colony formation in liquid culture between B7.2⁺ and B7.2⁻ KMS-27 cells (data not shown). Therefore, we investigated the expression of adhesion molecules (LFA-1, ICAM-1, very late antigen-4, vascular cell adhesion molecule-1), which might mediate the adhesion of myeloma cells to BM stroma cells and induce drug resistance (28, 29) on B7-H2⁺ and B7-H2⁻ KMS-27 cells. The expression levels of LFA-1 were much higher on B7-H2⁺ KMS-27 cells compared with those on B7-H2⁻ KMS-27 cells, although there was no difference in the expression of the other adhesion molecules (Fig. 3E).

Interaction between B7.2⁺ and B7-H2⁺ myeloma cells and CD4⁺ T cells confers a myeloma growth advantage. In the MLMR, normal CD4⁺ T cells were cultured with KMS-27 cells with or without anti-B7.2 and anti-ICOS mAbs. In a 5-day culture, either the anti-B7.2 or anti-ICOS mAb decreased the proliferation of CD4⁺ T cells and the combined use of these antibodies resulted in the maximum decrease (Fig. 4A). In other words, both B7.2 and B7-H2 molecules on KMS-27 cells stimulated CD4⁺ T-cell proliferation. The same result was obtained when fresh myeloma cells obtained from a plasma cell leukemia patient and expressing both B7.2 and B7-H2 molecules were used in the MLMR (Fig. 4B).

It was reported that B7.2 enhanced the production of Th1 and Th2 cytokines and that B7-H2 did not contribute to IL-2 induction (18, 19, 30). Consistent with these results, in MLMR using KMS-27 cells and CD4⁺ T cells, the mAb against B7.2 decreased the production of IL-10 as well as IFN-γ and IL-2. Meanwhile, the mAb against ICOS decreased the production of IL-10 and IFN-γ but not that of IL-2 (Supplementary Fig. S3). IL-4 was not detected in the supernatant of MLMR. The finding that both B7.2 and B7-H2 molecules on myeloma cells enhanced IL-10 production is particularly interesting because IL-10 not only reduces the antitumor immune response in general but also is a growth factor for myeloma cells.

Then, we examined whether soluble factors including IL-10 produced by the interaction between myeloma cells and CD4⁺ cells stimulate myeloma cell growth *in vitro*. First, we confirmed that when anti–IL-10 neutralizing antibody or control immunoglobulin was added to the KMS-27 cell culture, cell proliferation was not affected (Fig. 4C; data for control immunoglobulin are not shown). Furthermore, IL-10 was not detected in the supernatant of KMS-27 cell culture when examined using ELISA (data not shown). Therefore, KMS-27

cells themselves did not produce IL-10, but their proliferation was stimulated by exogenous IL-10 (Fig. 4C). Next, we cocultured using a transwell system, in which KMS-27 cells were plated onto a transwell membrane insert placed above the culture containing normal CD4$^+$ T cells with or without irradiated KMS-27 cells. The presence of irradiated KMS-27 cells in the lower cultures, compared with their absence, stimulated KMS-27 cell proliferation in the upper cultures (Fig. 4D, *two columns on the left*). Furthermore, this growth-promoting effect resulting from the CD4$^+$ T cell-irradiated KMS-27 cell interaction was eliminated partially or completely by adding anti-B7.2 mAb, anti-ICOS mAb, and/or anti-IL-10 neutralizing mAb to the lower cultures (Fig. 4D, *four columns on the right*). These results suggest that B7.2 or B7-H2 molecules on KMS-27 cells enhance CD4$^+$ T-cell proliferation and stimulate them to produce soluble factors, one of which, IL-10, enhances KMS-27 cell proliferation.

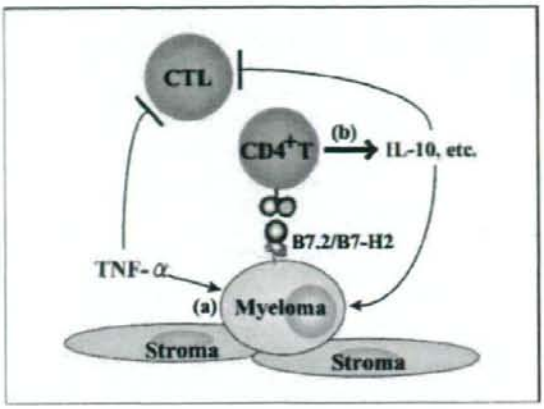

Fig. 5. New insight into myeloma biology based on the present data. *A*, in the BM environment, TNF-α and stromal cell contact induce B7.2 and B7-H2 molecule expression on myeloma cells. B7.2$^+$ and B7-H2$^+$ myeloma cells gain an intrinsic proliferative advantage. TNF-α also inhibits myeloma-specific CTLs. *B*, the B7.2 and B7-H2 molecules on myeloma cells induce CD4$^+$ T cells to produce soluble factors, one of which, IL-10, stimulates myeloma cell proliferation and inhibits myeloma-specific CTLs.

Discussion

The B7 family molecules stimulate or inhibit immune responses by costimulating or coinhibiting T cells. For example, in a mouse tumor model, B7-H2–expressing tumors increase the proliferation of tumor-specific CTLs (31). Meanwhile, the B7-H2-ICOS signal down-regulates the immune response in experimental animal models of autoimmune disease or acute graft-versus-host disease (32–34).

This study showed that the B7.2 expression levels on plasma cells were higher in MM patients compared with those in monoclonal gammopathy of unknown significance patients and hematologically normal individuals, and B7-H2 expression was detected in three MM patients alone but not in any monoclonal gammopathy of unknown significance patient or hematologically normal individual. Next, the expression of B7.2 and B7-H2 on MM cells was induced or enhanced by coculture with autologous stroma cells or by stimulation with TNF-α. Furthermore, myeloma cells expressing B7.2 and B7-H2 had increased cell cycling and more potential for proliferation. Finally, B7.2 and B7-H2 molecules on myeloma cells enhanced CD4$^+$ T-cell proliferation and stimulated them to produce soluble factors, one of which, IL-10, further stimulates the proliferation of myeloma cells.

B7.2 and B7-H2 molecules on myeloma cells were also involved in the production of other cytokines, IFN-γ and IL-2, which are known to enhance antitumor immune responses in general (35, 36). However, we and others observed that the expression of these molecules on acute myelogenous leukemia cells was associated with poor patient prognosis (21, 37). Similarly, lymphoma cells expressing B7.2 are associated with poor prognosis in a mouse lymphoma model (38). The effects of IFN-γ and IL-2, the production of which might be induced by B7.2 and B7-H2 molecules on myeloma cells, on the immunology and clinical behavior of MM should be clarified in further studies.

TNF-α, an immunomodulatory cytokine capable of inhibiting CTLs, is produced by the interaction between BM stroma cells and myeloma cells (39). It was shown that TNF-α directly stimulates myeloma cell growth *in vitro* and that serum TNF-α levels are higher in advanced-stage compared with early-stage MM patients (6, 7, 40). Based on our data presented here, we speculate that the TNF-α–induced growth advantage in myeloma may be, at least in part, associated with the induction of B7.2 and B7-H2 molecule expression on myeloma cells. The mechanism underlying the finding that myeloma cells expressing B7.2 and B7-H2 show increased cell cycling and greater potential to proliferate remains unknown. To the best of our knowledge, one previous report observed a similar phenomenon. Ghebeh et al. reported that high B7-H1 expression was correlated with high Ki-67 expression in tumor cells in breast cancer patients (41). In addition to this intrinsic advantage in cell proliferation of B7.2$^+$ and B7-H2$^+$ myeloma cells, these cells may obtain a further growth advantage by inducing the production of the myeloma-stimulatory cytokine IL-10 by CD4$^+$ T cells. It is well known that IL-10 inhibits the generation of tumor-specific CTLs (11, 12). We also confirmed that IL-10 inhibited the generation of KMS-27–specific CTLs *in vitro* (data not shown). This IL-10–mediated effect probably contributes further to myeloma cell growth. The above cascade of events is illustrated in Fig. 5. The IL-10 production induced by B7.2 and B7-H2 molecules is not myeloma specific because we observed that that AML cells expressing B7.2 and B7-H2 induced IL-10 production by CD4$^+$ T cells *in vitro*. It would be interesting to determine how broadly this mechanism works in a variety of human neoplasia.

The occurrence of immunologic derangement in MM supports the notion that modulation or normalization of this derangement would be beneficial for MM patients. Thalidomide and its analogues (e.g., lenalidomide), which have a variety of imunomodulatory activities, including potent inhibition of TNF-α production and stimulation of Th-1 immunity (42, 43), are effective in the treatment of MM patients. We speculate that full clarification of immunology in MM is the basis on which more specific, targeted therapy will be developed.

Disclosure of Potential Conflicts of Interest

No potential conflicts of interest were disclosed.

References

1. Massaia M, Dianzani U, Bianchi A, Camponi A, Boccadoro M, Pileri A. Defective generation of alloreactive cytotoxic T lymphocytes (CTL) in human monoclonal gammopathies. Clin Exp Immunol 1988; 73:214–8.
2. Cook G, Campbell JD, Carr CE, Boyd KS, Franklin IM. Transforming growth factor β from multiple myeloma cells inhibits proliferation and IL-2 responsiveness in T lymphocytes. J Leukoc Biol 1999;66:981–8.
3. Campbell JD, Cook G, Robertson SE, et al. Suppression of IL-2-induced T cell proliferation and phosphorylation of STAT3 and STAT5 by tumor-derived TGF β is reversed by IL-15. J Immunol 2001;167:553–61.
4. Hideshima T, Podar K, Chauhan D, Anderson KC. Cytokines and signal transduction. Best Pract Res Clin Haematol 2005;18:509–24.
5. Yasui H, Hideshima T, Richardson PG, Anderson KC. Novel therapeutic strategies targeting growth factor signalling cascades in multiple myeloma. Br J Haematol 2006;132:385–97.
6. Borset M, Waage A, Brekke OL, Helseth E. TNF and IL-6 are potent growth factors for OH-2, a novel human myeloma cell line. Eur J Haematol 1994;53:31–7.
7. Filella X, Blade J, Guillermo AL, Molina R, Rozman C, Ballesta AM. Cytokines (IL-6, TNF-α, IL-1α) and soluble interleukin-2 receptor as serum tumor markers in multiple myeloma. Cancer Detect Prev 1996;20:52–6.
8. Lu ZY, Zhang XG, Rodriguez C, et al. Interleukin-10 is a proliferation factor but not a differentiation factor for human myeloma cells. Blood 1995;85:2521–7.
9. Otsuki T, Yata K, Sakaguchi H, et al. IL-10 in myeloma cells. Leuk Lymphoma 2002;43:969–74.
10. Sadat-Sowti B, Debre P, Idziorek T, et al. A lectin-binding soluble factor released by $CD8^+CD57^+$ lymphocytes from AIDS patients inhibits T cell cytotoxicity. Eur J Immunol 1991;21:737–41.
11. Caux C, Massacrier C, Vanbervliet B, Barthelemy C, Liu YJ, Banchereau J. Interleukin 10 inhibits T cell alloreaction induced by human dendritic cells. Int Immunol 1994;6:1177–85.
12. de la Barrera S, Aleman M, Musella R, et al. IL-10 down-regulates costimulatory molecules on *Mycobacterium tuberculosis*-pulsed macrophages and impairs the lytic activity of CD4 and CD8 CTL in tuberculosis patients. Clin Exp Immunol 2004;138: 128–38.
13. Chen L, Linsley PS, Hellstrom KE. Costimulation of T cells for tumor immunity. Immunol Today 1993;14: 483–6.
14. Chen L, McGowan P, Ashe S, et al. Tumor immunogenicity determines the effect of B7 costimulation on T cell-mediated tumor immunity. J Exp Med 1994;179: 523–32.
15. Tamura H, Ogata K, Dong H, Chen L. Immunology of B7-1 and its roles in human diseases. Int J Hematol 2003;78:321–8.
16. Carreno BM, Carter LL, Collins M. Therapeutic opportunities in the B7/CD28 family of ligands and receptors. Curr Opin Pharmacol 2005;5:424–30.
17. Swallow MM, Wallin JJ, Sha WC. B7h, a novel costimulatory homolog of B7.1 and B7.2, is induced by TNFα. Immunity 1999;11:423–32.
18. Hutloff A, Dittrich AM, Beier KC, et al. ICOS is an inducible T-cell co-stimulator structurally and functionally related to CD28. Nature 1999;397:263–6.
19. Wang S, Zhu G, Chapoval AI, et al. Costimulation of T cells by B7-2, a B7-like molecule that binds ICOS. Blood 2000;96:2808–13.
20. Okamoto N, Tezuka K, Kato M, Abe R, Tsuji T. PI3-kinase and MAP-kinase signaling cascades in AILIM/ICOS- and CD28-costimulated T-cells have distinct functions between cell proliferation and IL-10 production. Biochem Biophys Res Commun 2003; 310:691–702.
21. Tamura H, Dan K, Tamada K, et al. Expression of functional B7-2 and B7.2 costimulatory molecules and their prognostic implications in *de novo* acute myeloid leukemia. Clin Cancer Res 2005;11:5708–17.
22. Pope B, Brown RD, Gibson J, Yuen E, Joshua D. B7-2-positive myeloma: incidence, clinical characteristics, prognostic significance, and implications for tumor immunotherapy. Blood 2000;96:1274–9.
23. Ogata K, Satoh C, Tachibana M, et al. Identification and hematopoietic potential of CD45- clonal cells with very immature phenotype ($CD45^-CD34^-$ $CD38^-Lin^-$) in patients with myelodysplastic syndromes. Stem Cells 2005;23:619–30.
24. Durie BG, Salmon SE. A clinical staging system for multiple myeloma. Correlation of measured myeloma cell mass with presenting clinical features, response to treatment, and survival. Cancer 1975;36:842–54.
25. Bataille R, Jégo G, Robillard N, et al. The phenotype of normal, reactive and malignant plasma cells. Identification of "many and multiple myelomas" and of new targets for myeloma therapy. Haematologica 2006;91: 1234–40.
26. Gimeno MJ, Maneiro E, Rendal E, Ramallal M, Sanjurjo L, Blanco FJ. Cell therapy: a therapeutic alternative to treat focal cartilage lesions. Transplant Proc 2005;37:4080–3.
27. Ogata K, Nakamura K, Yokose N, et al. Clinical significance of phenotypic features of blasts in patients with myelodysplastic syndrome. Blood 2002;100: 3887–96.
28. Asosingh K, Vankerkhove V, Van Riet I, Van Camp B, Vanderkerken K. Selective *in vivo* growth of lymphocyte function-associated antigen-1-positive murine myeloma cells. Involvement of function-associated antigen-1-mediated homotypic cell-cell adhesion. Exp Hematol 2003;31:48–55.
29. Schmidmaier R, Morsdorf K, Baumann P, Emmerich B, Meinhardt G. Evidence for cell adhesion-mediated drug resistance of multiple myeloma cells *in vivo*. Int J Biol Markers 2006;21:218–22.
30. Kuchroo VK, Das MP, Brown JA, et al. B7-1 and B7-2 costimulatory molecules activate differentially the Th1/Th2 developmental pathways: application to autoimmune disease therapy. Cell 1995;80:707–18.
31. Wallin JJ, Liang L, Bakardjiev A, Sha WC. Enhancement of $CD8^+$ T cell responses by ICOS/B7h costimulation. J Immunol 2001;167:132–9.
32. Wang G, Zhu L, Hu P, et al. The inhibitory effects of mouse ICOS-Ig gene-modified mouse dendritic cells on T cells. Cell Mol Immunol 2004;1:153–7.
33. Taylor PA, Panoskaltsis-Mortari A, Freeman GJ, et al. Targeting of inducible costimulator (ICOS) expressed on alloreactive T cells down-regulates graft-versus-host disease (GVHD) and facilitates engraftment of allogeneic bone marrow (BM). Blood 2005;105:3372–80.
34. Ansari MJ, Fiorina P, Dada S, et al. Role of ICOS pathway in autoimmune and alloimmune responses in NOD mice. Clin Immunol 2008;126:140–7.
35. Cheever MA, Greenberg PD, Fefer A, Gillis S. Augmentation of the anti-tumor therapeutic efficacy of long-term cultured T lymphocytes by *in vivo* administration of purified interleukin 2. J Exp Med 1982;155: 968–80.
36. Tuttle TM, McCrady CW, Inge TH, Salour M, Bear HD. γ-Interferon plays a key role in T-cell-induced tumor regression. Cancer Res 1993;53:833–9.
37. Maeda A, Yamamoto K, Yamashita K, et al. The expression of co-stimulatory molecules and their relationship to the prognosis of human acute myeloid leukaemia: poor prognosis of B7-2-positive leukaemia. Br J Haematol 1998;102:1257–62.
38. Stremmel C, Greenfield EA, Howard E, Freeman GJ, Kuchroo VK. B7-2 expressed on EL4 lymphoma suppresses antitumor immunity by an interleukin 4-dependent mechanism. J Exp Med 1999;189: 919–30.
39. Thalmeier K, Meissner P, Reisbach G, et al. Constitutive and modulated cytokine expression in two permanent human bone marrow stromal cell lines. Exp Hematol 1996;24:1–10.
40. Silvestris F, Cafforio P, Calvani N, Dammacco F. Impaired osteoblastogenesis in myeloma bone disease: role of upregulated apoptosis by cytokines and malignant plasma cells. Br J Haematol 2004;126:475–86.
41. Ghebeh H, Tulbah A, Mohammed S, et al. Expression of B7-H1 in breast cancer patients is strongly associated with high proliferative Ki-67-expressing tumor cells. Int J Cancer 2007;121:751–8.
42. Teo SK. Properties of thalidomide and its analogues: implications for anticancer therapy. AAPS J 2005;7: E14–9.
43. List AF. Lenalidomide—the phoenix rises. N Engl J Med 2007;357:2183–6.

Suppression of an Already Established Tumor Growing through Activated Mucosal CTLs Induced by Oral Administration of Tumor Antigen with Cholera Toxin[1]

Ayako Wakabayashi, Yohko Nakagawa, Masumi Shimizu, Keiichi Moriya, Yasuhiro Nishiyama, and Hidemi Takahashi[2]

Priming of CTLs at mucosal sites, where various tumors are originated, seems critical for controlling tumors. In the present study, the effect of the oral administration of OVA plus adjuvant cholera toxin (CT) on the induction of Ag-specific mucosal CTLs as well as their effect on tumor regression was investigated. Although OVA-specific TCRs expressing lymphocytes requiring in vitro restimulation to gain specific cytotoxicity could be detected by OVA peptide-bearing tetramers in both freshly isolated intraepithelial lymphocytes and spleen cells when OVA was orally administered CT, those showing direct cytotoxic activity without requiring in vitro restimulation were dominantly observed in intraepithelial lymphocytes. The magnitude of such direct cytotoxicity at mucosal sites was drastically enhanced after the second oral administration of OVA with intact whole CT but not with its subcomponent, an A subunit (CTA) or a B subunit (CTB). When OVA plus CT were orally administrated to C57BL/6 mice bearing OVA-expressing syngeneic tumor cells, E.G7-OVA, in either gastric tissue or the dermis, tumor growth was significantly suppressed after the second oral treatment; however, s.c. or i.p. injection of OVA plus CT did not show any remarkable suppression. Those mucosal OVA-specific CTLs having direct cytotoxicity expressed CD8$\alpha\beta$ but not CD8$\alpha\alpha$, suggesting that they originated from thymus-educated cells. Moreover, the infiltration of such OVA-specific CD8$^+$ CTLs was observed in suppressed tumor tissues. These results indicate that the growth of ongoing tumor cells can be suppressed by activated CD8$\alpha\beta$ CTLs with tumor-specific cytotoxicity via an orally administered tumor Ag with a suitable mucosal adjuvant. ***The Journal of Immunology*****, 2008, 180: 4000–4010.**

Many malignant tumors originate from various epithelial tissues such as the skin or mucosal sites such as the esophagus, stomach, colon, or lung (1). Thus, as a cancer vaccine, it is essential to stimulate mucosal or dermal immune systems, as well as the systemic immune system, with a suitable Ag, adjuvant, and administration route as reviewed by Finn (2). Mucosal immunization using an adjuvant that enables the priming of both mucosal and systemic immunity (3, 4) may be a good way to prevent or treat mucosal tumors. In particular, the induction of mucosal CTLs that can specifically recognize tumor-derived peptide Ags presented by the corresponding class I MHC molecules seems to be one of the most important issues for eliminating tumor cells (5).

In the mucosal compartment, lymphocytes located in the intestinal epithelium are almost exclusively T cells called intraepithelial lymphocytes (IELs)[3] (3). Such IELs are mostly CD8$^+$ T cells that are classified into three distinct populations: TCR$\alpha\beta^+$CD8$\alpha\beta^+$, TCR$\alpha\beta^+$CD8$\alpha\alpha^+$, and TCR$\gamma\delta^+$CD8$\alpha\alpha^+$ (6). IELs contain cytotoxic properties and specifically eliminate virus- or parasite-infected cells (7–9); however, although spontaneous cytotoxicity of human IELs against tumor cells has been reported (10, 11), their actual specificity on tumors is still unknown. Recently, we have reported (12) that a marked increase in the number of HIV-1-specific CD8$\alpha\beta$-positive T cells among IELs was observed in HIV-1-specific TCR transgenic (Tg) mice when they received intrarectal or i.p. administration of the recombinant vaccinia virus (rVV) expressing a known restricted CTL epitope, P18 (rVV-P18), which is restricted by H-2D^d-class I MHC molecules (13). Using H-2D^d/P18 tetramers, we could detect CD8-positive, P18-specific TCR-expressing T cells in freshly isolated IELs and splenic T cells of unchallenged naive Tg mice. Although those H-2D^d/P18 tetramer-positive CD8 T cells from naive Tg mice did not show any specific cytotoxicity, freshly isolated mucosal T cells bearing CD8$\alpha\beta$ but not CD8$\alpha\alpha$ from activated Tg mice with rVV-P18 represented P18-specific cytotoxicity against tumor cells expressing the epitope, and the magnitude of cytotoxicity was much stronger than that in activated splenic T cells (12). These results suggest that in vivo activated mucosal CD8$\alpha\beta$ CTLs with tumor-specific cytotoxicity may be critical for controlling tumors expressing the specific epitope in vivo rather than systemic splenic CTLs.

Cholera toxin (CT) derived from *Vibrio cholerae* is known as a potent mucosal adjuvant comprised of one toxic A subunit (CTA) with ADP-ribosyltransferase activity and five nontoxic B subunits (CTB) responsible for binding to monosialoganglioside (GM) 1 on the cell surface (14, 15). CT adjuvant helps to produce both systemic IgG and mucosal IgA (16) as well as to induce Ag-specific

Department of Microbiology and Immunology, Nippon Medical School, Tokyo, Japan

Received for publication April 13, 2007. Accepted for publication January 7, 2008.

The costs of publication of this article were defrayed in part by the payment of page charges. This article must therefore be hereby marked *advertisement* in accordance with 18 U.S.C. Section 1734 solely to indicate this fact.

[1] This work was supported in part by Grants-in-Aid for Young Scientists from the Japan Society for the Promotion of Sciences, from the Ministry of Education, Science, Sport, and Culture, from the Ministry of Health and Labor and Welfare, Japan, and from the Promotion and Mutual Aid Corporation for Private Schools of Japan.

[2] Address correspondence and reprint requests to Dr. Hidemi Takahashi, Department of Microbiology and Immunology, Nippon Medical School, 1-1-5 Sendagi, Bunkyo-ku, Tokyo 113-8602, Japan. E-mail address: htkuhkai@nms.ac.jp

[3] Abbreviations used in this paper: IEL, intraepithelial lymphocyte; CT, cholera toxin; CTA, CT A subunit (toxic); CTB, CT B subunit (nontoxic); DC, dendritic cell; GM, monosialoganglioside; *Hp*, *Helicobacter pylori*; LPL, lamina propria lymphocyte; MadCAM-1, mucosal addressin cell-adhesion molecule-1; OVA-CT, CT-conjugated OVA; PP, Peyer's patch; rVV, recombinant vaccinia virus; SC, spleen cell; Tg, transgenic; TIL, tumor-infiltrating lymphocyte.

$CD4^+$ T cell responses in the spleen, reflecting the systemic compartment, and in Peyer's patches (PPs), reflecting the mucosal compartment (17). In addition, it has been demonstrated (18) that OVA-specific CTLs could be primed in C57BL/6 mice following oral exposure to a combination of OVA with CT, and specific cytotoxic activity was detected from spleen cells (SCs) only when they were restimulated in vitro with irradiated OVA-expressing syngeneic tumor cells, E.G7-OVA, which are OVA gene-transfected EL4 thymoma cells (19, 20). Also, intranasal preimmunization with OVA peptide (SIINFEKL) plus CT primed similar OVA-specific CTLs in the spleen of C57BL/6 mice, and the immunized mice were protected from the development of transferred E.G7-OVA (21).

Moreover, it has been shown that adoptive transfer of naive $CD8^+$ OVA-specific OT-I T cells into E.G7-OVA tumor-bearing syngeneic mice did not inhibit tumor growth, although adoptive transfer of preactivated OT-I CTL in vitro inhibited tumor growth in a dose-dependent manner (22). Furthermore, it has recently been reported that vaccination with dendritic cells (DCs) prepulsed ex vivo with CT-conjugated OVA (OVA-CT) gave rise to OVA-specific splenic $CD8^+$ T cells that produced IFN-γ, were cytotoxic to E.G7-OVA cells in vivo, and rejected already established in vivo E.G7-OVA tumors associated with high numbers of tumor-infiltrating $CD8^+$ T cells (23), indicating that the elimination of previously established tumor cells might require the infiltration of tumor-specific activated $CD8^+$ CTLs.

In the present study, we found two distinct types of $CD8\alpha\beta$-positive T cells among freshly isolated lymphocytes expressing OVA-specific TCRs, which can be detected by OVA peptide-bearing tetramers. One is in an activated effector state with cytotoxic activity and the other is a resting state and may gain cytotoxicity when stimulated with an OVA epitope peptide in vitro. Based on the observations, we defined direct cytotoxicity as the former state, in which freshly isolated and unstimulated CD8 T cells had specific cytotoxicity. Therefore, by comparing systemic SCs, we asked whether OVA-specific cytotoxic activity could be observed among freshly isolated IELs in mice orally administered OVA plus CT and examined whether those activated CTLs would reject or suppress the growth of already established tumors. Consequently, we observed dominant $TCR\alpha\beta$ and $CD8\alpha\beta$ OVA-specific CTL activities in freshly isolated IELs rather than in SCs after the oral administration of OVA plus CT, and such mucosal CTL activities could be expanded after oral boosting. Moreover, the growth of E.G7-OVA inoculated into the stomach or the epidermis was significantly suppressed, accompanied by the expansion of activated mucosal CTLs, and the infiltration of such OVA-specific $CD8\alpha\beta^+$ CTLs was observed in suppressed dermal tumor tissues. These results indicate that the growth of ongoing tumor cells can be suppressed in vivo by activated $CD8\alpha\beta$ CTLs with tumor-specific cytotoxicity via an orally administered tumor Ag with a suitable mucosal adjuvant.

Materials and Methods

Mice

Six- to 8-wk-old female C57BL/6 ($H\text{-}2^b$) mice were purchased from Charles River Japan, maintained in microisolator cages under pathogen-free conditions, and fed autoclaved laboratory chow and water. All animal experiments were performed according to guidelines for the care and use of laboratory animals set by the National Institutes of Health (NIH; Bethesda, MD) and approved by the Review Board of Nippon Medical School (Tokyo, Japan).

Oral and systemic immunization

Chicken egg OVA, grade V (Sigma Aldrich), was dissolved in sterilized PBS. Mice were orally administered 100 mg of OVA or 10 μg of CT (List Biological Laboratories) alone or 100 mg of OVA plus 10 μg of CT, CTA, or CTB (List Biological Laboratories) in 0.3 ml of PBS. In some experiments, mice were orally administered 10 mg of OVA plus 10 μg of CT. For systemic immunization, mice were i.p. or s.c. injected with 100 mg of OVA or the same dose of OVA plus 10 μg of CT.

Preparation of IELs, lamina propria lymphocytes (LPLs), SCs, and tumor-infiltrating lymphocytes (TILs)

IELs were prepared by the method described previously (12). In brief, after the small intestine, large intestine, or stomach was obtained from mice, fecal materials were flushed from the lumen with HBSS (Invitrogen Life Technologies) and connective tissues were carefully removed. The obtained guts were inverted and cut into several segments that were transferred to a 50-ml conical tube (Becton Dickinson Labware) containing 45 ml of HBSS with 5% FCS, 100 U/ml penicillin (Invitrogen Life Technologies), and 100 μg/ml streptomycin (Invitrogen Life Technologies). The tube was then shaken at 37°C for 45 min (horizontal position; orbital shaker at 150 rpm). Harvested cells from the intestinal epithelium were passed through a 10-ml syringe column containing loosely packed glass wool to remove tissue debris. Subsequently, the cells were suspended in 30% Percoll solution (Amersham Biosciences) and centrifuged for 20 min at 1,800 rpm. Cells at the bottom of the solution were then subjected to Percoll discontinuous gradient centrifugation for 20 min at 1,800 rpm and IELs were recovered at the interphase of 44 and 70% Percoll solutions. LPLs were prepared by the method described previously (24). In brief, after the small intestine, large intestine, or stomach was dissected from mice, fecal material was flushed from the lumen with HBSS and PPs were carefully removed. The obtained guts were inverted and cut into several segments that were transferred to a 50-ml conical tube containing 45 ml of HBSS with 5% FCS and 1 mM EDTA (Wako Pure Chemical Industries). The tube was shaken at 37°C for 45 min (horizontal position; orbital shaker at 150 rpm). The gut segments were then washed with PBS and shaken in 40 ml of HBSS with 5% FCS and 0.1 mg/ml collagenase (Sigma-Aldrich) at 37°C for 45 min (horizontal position; orbital shaker at 60 rpm). Harvested cells were passed through a nylon mesh and suspended in 40% Percoll solution, and then 70% Percoll solution was underlain. The solution was centrifuged for 20 min at 1,800 rpm and LPLs were recovered at the interphase of 40 and 70% Percoll solutions. These procedures provided >95% viable lymphocytes with a cell yield of $5\text{–}10 \times 10^6$ of small intestinal IELs, $2\text{–}3 \times 10^5$ of large intestinal IELs, $7\text{–}12 \times 10^3$ of gastric IELs, $4\text{–}9 \times 10^5$ of small intestinal LPLs, $1\text{–}3 \times 10^5$ of large intestinal LPLs, or $5\text{–}9 \times 10^4$ of gastric LPLs per mouse. The cells were suspended in complete T cell medium (25) composed of RPMI 1640 medium (Sigma-Aldrich) supplemented with 2 mM L-glutamine (ICN Biomedicals), 1 mM sodium pyruvate (Invitrogen Life Technologies), 0.1 mM nonessential amino acid (Invitrogen Life Technologies), a mixture of vitamins (ICN Biomedicals), 1 mM HEPES (Invitrogen Life Technologies), 100 U/ml penicillin (Invitrogen Life Technologies), 100 μg/ml streptomycin (Invitrogen Life Technologies), 50 μM 2-ME (Sigma-Aldrich), and heat-inactivated 10% FCS. For TIL preparation, tumors were removed from mice, incubated in 1 mg/ml collagenase (Wako Pure Chemical Industries) with PBS at 37°C for 1 h, and crushed gently. TILs were prepared using Percoll solutions as described in the previous paragraph regarding IEL preparation. The spleen was aseptically removed and a single cell suspension was prepared. For osmotic hemolysis, single cells were suspended in 0.1× PBS and an equal amount of 2× PBS was added immediately. To enrich IELs, LPLs, and TILs from mice, the interface between the 40 and 70% Percoll solutions (26), in which NK cells and unfractionated SCs, which may also include NK cells, must be included, was collected.

Flow cytometry analysis

Cells were double-stained with PE-labeled $H\text{-}2K^b$/OVA tetramer-SIINFEKL (Beckman Coulter) or $H\text{-}2K^b$/PB1 tetramer-SSYRRPVGI (Medical & Biological Laboratories) and FITC-labeled anti-mouse TCRβ, CD8α (BD Pharmingen), or CD8β (Caltag Laboratories). Peptide PB1 703–711, SSYRRPVGI, for the control tetramer was derived from influenza virus (27). Dead cells were determined using 7-aminoactinomycin D viability dye (Beckman Coulter) and stained cells were analyzed by FACScan using the CellQuest program (BD Biosciences).

In vitro restimulation of SCs or IELs with E.G7-OVA

Lymphocytes were restimulated in vitro by the method described previously (19). Freshly isolated SCs (3×10^7) or IELs (3×10^7) were restimulated with 3×10^6 irradiated (20,000 rad) E.G7-OVA cells (19, 20) ($H\text{-}2^b$; American Type Culture Collection) in 10 ml of complete T cell medium per upright 25-cm^2 flask in 5% CO_2 at 37°C for 6 days. Six days later, the viability of the lymphocytes was 35–51% in SCs and 16–26% in IELs. The

in vitro restimulated cells were collected and their OVA-specific cytotoxicity was measured by the following procedure.

CTL assay

For the CTL assay, freshly isolated IELs, SCs, or TILs were used. Cytolytic activity was measured using a standard ^{51}Cr-release assay as previously described (12). In brief, various numbers of effector cells were incubated with 3×10^3 ^{51}Cr-labeled targets for 6 h at 37°C in 200 μl of RPMI 1640 medium containing 10% FCS in round-bottom 96-well cell culture plates (BD Biosciences). After incubation, the plates were centrifuged for 10 min at $330 \times g$, and 100 μl of cell-free supernatants were collected to measure radioactivity with a Packard Auto-Gamma 5650 counter (Hewlett-Packard Japan). Maximum release was determined from the supernatant of cells that had been lysed by the addition of 5% Triton X-100, and spontaneous release was determined from target cells incubated without added effector cells. The percentage of specific lysis was calculated as 100 × (experimental release − spontaneous release)/(maximum release − spontaneous release). SEs of the means of triplicate cultures were always <5% of the mean. Each experiment was performed at least three times.

Measurement of in vivo antitumor effects

E.G7-OVA cells (5×10^6), OVA gene-transfected EL4 thymoma cells (19, 20), were implanted into the gastric or dermal tissue of syngeneic C57BL/6 mice (H-2^b). For tumor implantation into the gastric tissue, mice were anesthetized and underwent an abdominal operation and then E.G7-OVA cells in 50 μl of RPMI 1640 were injected into the muscle layer of the stomach using a syringe with a 29-gauge needle (Terumo). For implantation into the dermal tissue, mice were anesthetized and E.G7-OVA cells in 100 μl of RPMI 1640 were injected intradermally by a 29-gauge needle syringe. On day 3 after implantation into the gastric or dermal tissue, when the tumor mass became visible, tumor-bearing mice were orally or systemically administered OVA plus CT as described above. Seven days after the first administration, some of the mice were similarly boosted with the same materials. The growing tumors implanted into the gastric or dermal tissues were followed by measuring the length (a) and width (b), the and tumor volume (V) was calculated according to the formula $V = ab^2/2$ as reported previously (28). When the longer axis of each tumor was >20 mm, all mice were anesthetized and sacrificed according to the guidelines for the care and use of laboratory animals set by the NIH.

Histological analysis of tumor tissues

Freshly excised tumor tissues were embedded in Tissue-Tek OCT compound (Sakura Finetek) at −80°C. Tissue segments were sectioned at 6 μm using a cryostat. Sections were placed on a poly-L-lysine-coated glass slide, air dried, and then fixed in 10% formalin PBS for 5 min and stained with H&E. For immunohistochemical staining, sections were fixed in cold acetone for 5 min and incubated with blocking solution (Block-ace; Dainippon Pharmaceutical) for 30 min at 37°C and then incubated with biotin-conjugated rat anti-CD8β Ab (Caltag Laboratories) or control isotype-matched rat IgG2a Ab (Caltag Laboratories) overnight at 4°C. Endogenous peroxidase was quenched by incubation in 0.3% H_2O_2 and 0.1% NaN_3 in distilled water for 10 min. The sections were incubated with avidin-biotin peroxide complexes (Vectastain ABC kit; Vector Laboratories) followed by color reaction with a Vectastain diaminobenzidine substrate kit (Vector Laboratories).

Statistical analysis

Student's t test was used to determine the statistical significance of differences between groups in tumor growth. Data were considered significant at $p < 0.05$.

Results

Priming of OVA-specific CD8$\alpha\beta$-positive CTLs with direct cytotoxicity via oral administration with OVA plus CT

It has been reported that OVA-specific CTLs could be primed in C57BL/6 mice by oral or i.v. immunization with OVA plus CT together with nontoxic CTB, and specific cytotoxic activity was detected from immune SCs only when they were restimulated in vitro with irradiated OVA-expressing syngeneic tumor (E.G7-OVA) cells (18). It has also been shown that activated CTLs but not naive primed CTLs could represent antitumor responses in vivo (22). Similarly, we have recently observed in HIV-1-specific CTL-TCR transgenic mice that activated CTLs but not freshly isolated TCR-bearing CD8$\alpha\beta$-positive T cells showed specific cytotoxicity, and the most critical sites for activating TCR-bearing CD8$\alpha\beta$ T cells were mucosal compartments when Tg mice were administered a specific Ag for TCR (12).

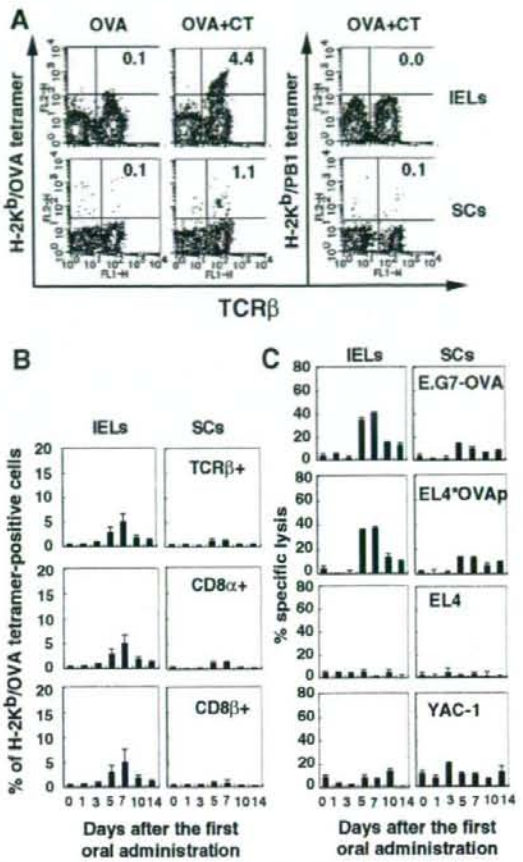

FIGURE 1. Analysis of OVA-specific direct cytotoxicities in IELs and SCs after primary immunization with OVA plus CT. *A*, Analysis of H-2K^b/OVA tetramer-positive cells. C57BL/6 mice were orally administered OVA or OVA plus CT once. IELs and SCs were collected from mice 5 days after the first oral administration, stained with either PE-labeled H-2K^b/OVA tetramer-SIINFEKL or H-2K^b/PB1 tetramer-SSYRRPVGI together with FITC-labeled anti-mouse TCRβ, and analyzed by flow cytometry. Each value represents the percentage of cells expressing both indicated markers. Data are representative of three independent experiments. *B*, Kinetics of H-2K^b/OVA tetramer-positive cells after primary immunization. C57BL/6 mice were orally administered OVA plus CT once. IELs and SCs were collected from mice at various days after the first oral administration, stained with PE-labeled H-2K^b/OVA tetramer together with FITC-labeled anti-mouse TCRβ, CD8α, or CD8β, and analyzed by flow cytometry. The results are shown as the mean ± SD of four mice. *C*, Kinetics of OVA-specific direct cytotoxic responses. C57BL/6 mice were orally primed and cells were collected as described in *B*. OVA-specific CTL responses were measured by ^{51}Cr-release assay using E.G7-OVA cells (H-2^b), YAC-1 cells, and EL4 cells (H-2^b) pulsed with or without 4 μM OVA-peptide, SIINFEKL, as target cells. E:T ratio was 100:1. The results shown as the mean ± SD in triplicate of pooled cells from two mice are representative of three independent experiments.

These findings prompted us to examine whether direct OVA-specific cytotoxic activity could be induced among IELs in mice

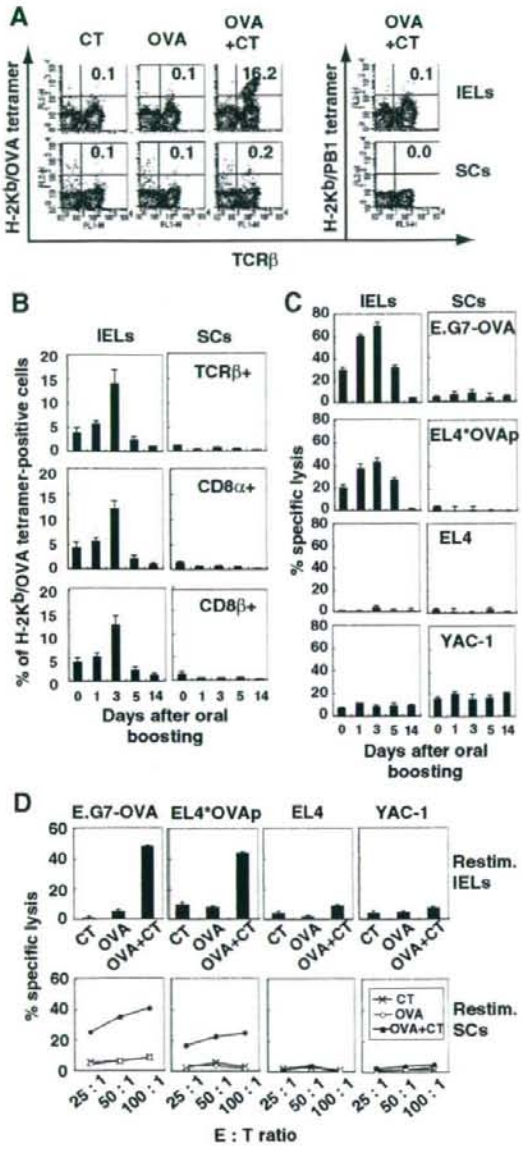

FIGURE 2. Expansion of direct OVA-specific cytotoxicities after oral boosting with OVA plus CT. *A*, Activated H-2K^b/OVA tetramer-positive cells after oral boosting. C57BL/6 mice were orally administered CT, OVA, or OVA plus CT once weekly for 2 wk. IELs and SCs were collected from mice 3 days after the second oral boost and stained with PE-labeled H-2K^b/OVA tetramer or H-2K^b/PB1 tetramer together with FITC-labeled anti-mouse TCRβ. Each value represents the percentage of cells expressing both indicated markers. Data are representative of three independent experiments. *B*, Kinetics of H-2K^b/OVA tetramer-positive cells after oral boosting. C57BL/6 mice were orally administered OVA plus CT once weekly for 2 wk. IELs and SCs were collected from mice at various days after the second oral boost, stained with PE-labeled H-2K^b/OVA tetramer together with FITC-labeled anti-mouse TCRβ, CD8α, or CD8β, and analyzed by flow cytometry. The results are shown as the mean ± SD of four mice. *C*, Kinetics of the secondary expansion of OVA-specific direct CTL responses. C57BL/6 mice were treated orally and the cells were collected as described in *B*. OVA-specific CTL responses were measured by ^{51}Cr-release assay using E.G7-OVA cells, YAC-1 cells, and EL4 cells pulsed with or without OVA peptide as targets. The E:T ratio is 100:1. The results shown as the mean ± SD in triplicate of pooled cells from two mice are representative of three independent experiments. *D*, Activation of OVA-specific CTLs by in vitro restimulation (Restim.). C57BL/6 mice were orally administered CT, OVA, or OVA plus CT once weekly for 2 wk. IELs (3×10^7) and SCs (3×10^7) were collected from mice 9 days after the second oral boost, and cocultured with 3×10^6 irradiated E.G7-OVA. Six days later, OVA-specific lysis of stimulated IELs and SCs was measured by ^{51}Cr-release assay. The E:T ratio is 100:1 in IELs and 100:1, 50:1, or 25:1 in SCs. The results are shown as the mean ± SD in IELs or the mean in SCs in triplicate of pooled cells from two mice. Data are representative of three independent experiments.

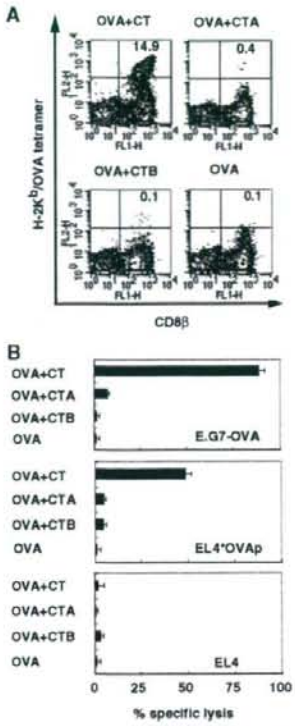

FIGURE 3. Both subunits, CTA and CTB, are essential for the induction of OVA-specific CTLs. C57BL/6 mice were orally administered OVA or OVA plus intact CT, CTA subunit or CTB subunit once weekly for 2 wk. IELs were collected from mice 3 days after the second oral administration. *A*, IELs were stained with PE-labeled H-2K^b/OVA tetramer and FITC-labeled anti-mouse CD8β. Each value represents the percentage of cells expressing both indicated markers. *B*, OVA-specific CTL responses of isolated IELs were measured by ^{51}Cr-release assay using E.G7-OVA cells, EL4 cells pulsed with or without OVA peptide as targets. The E:T ratio is 100:1. Data are shown as the mean ± SD in triplicate of pooled cells from two mice. The results are representative of three independent experiments for both *A* and *B*.

administered OVA plus CT orally without requiring in vitro restimulation. To carry out this experiment, we used a H-2K^b/OVA tetramer to detect cells expressing OVA-specific TCR in freshly isolated IELs as well as in the SCs of primed mice 5 days after immunization. Also, to evaluate the purity of IELs, CD103 (integrin